

[Click here to view linked References](#)

1 Source patterns of Potentially Toxic Elements (PTEs) and mining activity 2 contamination level in soils of Taltal city (Northern Chile)

3 Arturo Reyes^{1,2,a}, Matar Thiombane^{3,4,a,b}, Antonio Panico⁵, Linda Daniele⁶, Annamaria Lima³,
4 Marcello Di Bonito⁷, Benedetto De Vivo^{4,5}

5 ¹ Departamento de Ingeniería en Minas. Universidad de Antofagasta, Antofagasta. Chile

6 ² Centro de Investigación Científico Tecnológico para la Minería, CICITEM, Antofagasta, Chile

7 ³ Dipartimento di Scienze della Terra, dell'Ambiente e delle Risorse, Università degli Studi di Napoli
8 "Federico II", Complesso Universitario Monte S. Angelo, Via Cintia snc, 80126 Naples, Italy

9 ⁴ Norwest Italia Srl, 80138, Napoli, Italy

10 ⁵ Pegaso University, Piazza Trieste e Trento 48, 80132 Naples, Italy

11 ⁶ Departamento de Geología, Universidad de Chile – Plaza Ercilla 803 – Santiago, Chile

12 ⁷ School of Animal, Rural and Environmental Sciences, Brackenhurst Campus Southwell NG25 0QF
13 Nottingham Trent University, United Kingdom

14

15 ^a First authors with equal contribution

16 ^b Corresponding author. E-mail address: thiombane.matar@unina.it (M. Thiombane)

17

18 Highlights

- 19 • High concentrations of PTEs are displayed in the north-eastern part of Taltal city
- 20 • Abandoned mining waste deposits are the main source of PTEs in the study area
- 21 • Very high contamination level is displayed in soils nearby mining waste deposit (S1)

22

23

24 Abstract

25 Mining activities are amongst the main sources of Potentially Toxic Elements (PTEs) in the environment
26 which constitute a real concern worldwide, especially in developing countries. These activities have
27 been carried out for more than a century in Chile, South America, where, as evidence of incorrect waste
28 disposal practices, several abandoned mining waste deposits were left behind. This study aimed to
29 understand multi-elements geochemistry, source patterns and mobility of PTEs in soils of the Taltal
30 urban area (northern Chile). Topsoil samples (n = 125) were collected in the urban area of Taltal city (6
31 km²) where physicochemical properties (Redox potential, Electric conductivity and pH) as well as
32 chemical concentrations for 35 elements were determined by inductively coupled plasma optical
33 emission spectrometer (ICP-OES). Data were treated following a robust workflow, which included Factor
34 Analysis (based on \ln -transformed data), a new Robust Compositional Contamination Index (RCCI), and
35 Fractal/multi-fractal interpolation in GIS environment. This approach allowed to generate significant

36 elemental associations, identifying pool of elements related either to the geological background,
37 pedogenic processes accompanying soil formation or to anthropogenic activities. In particular, the study
38 eventually focused on a pool of 6 PTEs (As, Cd, Cr, Cu, Pb, and Zn), their spatial distribution in the
39 Taltal city, and the potential sources and mechanisms controlling their concentrations. Results showed
40 generally low baseline values of PTEs in most sites of the surveyed area. On a smaller number of sites,
41 however, higher values concentrations of As, Cd, Cu, Zn and Pb were found. These corresponded to
42 very high RCCI contamination level, and were correlated to potential anthropogenic sources, such as
43 the abandoned mining waste deposits in the north-eastern part of the Taltal city. This study highlighted
44 new and significant insight on the contamination levels of Taltal city, and its links with anthropogenic
45 activities. Further research is considered to be crucial to extend this assessment to the entire region.
46 This would provide a comprehensive overview and vital information for the development of intervention
47 limits and guide environmental legislation for these pollutants in Chilean soils.

48
49

50 **Keywords:** Taltal city; Chile; Mining waste deposits; PTEs; contamination level; RCCI

51

52 **1. Introduction**

53 Environmental geochemistry aims to reveal inorganic elements sources and discriminate anthropogenic
54 pollution to natural (geogenic) source (Lima et al., 2003; Albanese et al., 2007; Reimann et al., 2008)
55 which can release contaminants into atmospheric, soil and water media (Prapamontol and Stevenson,
56 1991; Suchan et al., 2004). Industrial activities, domestic, livestock and municipal wastes,
57 agrochemicals, and petroleum-derived products can all be sources of chemicals and contaminants
58 (Reimann and De Caritat, 2005; Luo et al., 2009; Bundschuh et al., 2012). However, some sources of
59 potentially toxic elements (PTEs) and contamination in urban area might be also related to geogenic
60 (i.e., natural) backgrounds (Cicchella et al., 2005; Biasioli et al., 2007; Luo et al., 2012). In fact, several
61 soil parent materials are natural sources of PTEs, which can pose a risk to the environment and human
62 health when at elevated concentrations. Urban soil pollution is one of the most challenging
63 environmental issues to tackle due to its impact to human health and the ecosystem (Cicchella et al.,
64 2005; Albanese et al., 2010; Petrik et al., 2018a). In addition, PTEs are increasing due to accelerated
65 population growth rate, higher level of urbanisation and industrialisation, providing a great variety of
66 anthropogenic contamination/pollution sources (Wang et al., 2012; Wu et al., 2015; Guillén et al., 2017).
67 In order to address these challenges, a variety of geostatistical computations and mapping tools have
68 been developed and used to identify sources and patterns of different PTEs, to isolate their provenance

69 compared to underlying geological features and/or anthropogenic activities (Albanese et al., 2007;
70 Reimann et al., 2008, Thiombane et al., 2018a), and therefore assess the potential contamination levels
71 in a meaningful way. A Large number of indices aimed to quantify contamination levels into
72 environment, such as the Enrichment factors (Chester and Stoner, 1973), the Geoaccumulation Index
73 (Müller, 1969) and the Single Pollution Index (Hakanson, 1980; Müller, 1981). But, authors such
74 Reimann and de Caritat (2000, 2005), Petrik et al. (2019) have clearly demonstrated that indices (e.g.,
75 Enrichment factor and Pollution Index) using background/baseline values for reference) “are
76 straightforward, but are not scale-invariant, which means that changes in units of the measured
77 concentrations will modify the results of the analysis” (Aitchison and Egozcue, 2005; Pawlowsky-Glahn
78 and Buccianti, 2011; Pawlowsky-Glahn et al., 2015). Moreover, Element ratio variations and Enrichment
79 factors (EFs) values can vary depending on the different parent rock materials and chosen reference
80 media as well as reference elements (Reimann and de Caritat, 2000; 2005). In addition, these indices
81 do not take into account the different biogeochemical processes, the natural fractionation of elements or
82 differential solubility of minerals (Sucharovà et al., 2012) which may have remarkable impact on
83 elemental enrichment/contamination (Reimann and de Caritat, 2000, 2005). In order to address some of
84 these issues, Petrik et al. (2018a) introduced a new contamination index called Robust Compositional
85 Contamination Index (RCCI) that considers the compositional structure of the data (Aitchison and
86 Egozcue, 2005; Pawlowsky-Glahn and Buccianti, 2011; Pawlowsky-Glahn et al., 2015) avoiding outlier's
87 artefacts.

88 Among anthropogenic activities, mining activity is considered a major environmental issue worldwide,
89 especially in developing countries (Ezeigbo and Ezeanyim, 1993; Lim e al., 2008; Naicker et al., 2003;
90 Azevedo-Silva et al., 2016) due to releases of mining tailings and polluted wastewater into soils,
91 atmosphere and hydrosphere and their long-lasting consequences. Such mining activities have been
92 carried out for a long time in Chile. In particular, over the past 100 years they were intensified by the
93 industrial acceleration, leaving behind a plethora of testimonies of incorrect waste disposal practices,
94 including several abandoned sites containing mining waste with elevated concentrations of PTEs. This
95 situation is particularly serious in the region of Antofagasta, northern Chile, characterized by the
96 presence of a high density of mining operations. A case study of great concern is the Taltal city
97 (Antofagasta region), where the CENMA (2014) has reported the occurrence of a large number of Cu
98 and Au-related abandoned mining waste deposits in its proximity. Over the years, the Taltal city has
99 considerably expanded, causing uncontrolled urbanisation, encroaching these abandoned sites of
100 mining wastes that may be a real concern for local population directly exposed to PTEs-related mining
101 tailings. The main aim of this study is to identify possible contamination impacts of these abandoned
102 mining waste deposits in soils of the Taltal city. In order to achieve this aim, the main objectives are:

- 103 (1) To measure multi-elements concentration level in soils of the Taltal city, and their spatial
104 distributions in the study area;
- 105 (2) To determine the background/baseline concentration of 6 PTEs;
- 106 (3) To quantify the effect of abandoned mining waste deposits in soils of the Taltal city, and
- 107 (4) To assess the contamination level in topsoil of Taltal urban area, based on a robust compositional
108 index of the 6 considered PTEs

109 This study presents an analysis of the spatial abundance of 6 PTEs in soils of Taltal city which will be
110 assessed by applying the new RCCI that honours the compositional structure of the data. This survey is
111 important because it constitutes the first study carried out on soils of Taltal city and can be considered a
112 stepping stone towards a more detailed and meaningful investigation on potential sources and levels of
113 PTEs in this area. Further research would be crucial to extend the same approach to the entire region,
114 to provide vital information for future developments of environmental legislation for defining intervention
115 limits of these pollutants in Chilean soils.

116

117 **2. Materials and methods**

118 **2.1. Geological features and landuse of the study area**

119 The Taltal Municipality, covering an area of about 20,400 km², is located in northern Chile, in the
120 southern part of the Antofagasta region, within the Atacama Desert, and bordered on its western part by
121 the Pacific Ocean (Fig. 1A).

122 **[Figure 1 about here]**

123

124 The main geological features of the Taltal municipality are constituted by two volcanic deposits called
125 “La Negra” formations, consisting of volcanic clasts (andesitic and andesitic-basaltic lavas) with
126 intercalations of sandstones (sandstones, tuffites and breccia, fine-grained to locally calcareous,
127 composed by volcanic clasts) (Escribano et al., 2013) (Fig. 1B). They shape two major mountainous
128 geomorphologic domains: the Coastal Range, which can reach elevations up to 2,650 m and the
129 Coastal Scarp, reaching up to 1,000 m (Escribano et al., 2013). Within these two geological features
130 there intrude the “Aeropuerto” formation, composed of porphyritic, banded rhyolite with plagioclase,
131 quartz and spherulite phenocrysts with a small outcrop. This covers a surface of more than 1.5 km² in
132 the north of the Taltal city and crosses the area with a NW-SE orientation. The area surveyed by this
133 study (Taltal city) is mostly consisting of the eroded products of the “Negra” formation deposit, including
134 alluvial and colluvial deposits containing mixed conglomerates, sandstones, breccia, and marine
135 sedimentary sequence, whose underline part is composed of calcareous sandstones, mudstones and

136 fossiliferous shales (Triassic-Early Jurassic, Escribano et al., 2013). Along the coast, outcrops of marine
137 deposits, conglomerate, and calcareous sandstone dominate the geological features, where a
138 succession of marine abrasion terraces and littoral cords can be found (Escribano et al., 2013).
139 The study was carried out in the main urban area of the Taltal municipality which hosts more than
140 17,000 inhabitants, where around 89% of the population is grouped in Taltal city, located in the Atacama
141 Desert. The climate of the area is characterised by an annual average temperature of 18 °C, almost
142 total lack of precipitation and only occasional torrential rainfalls fall during the autumn season
143 accompanied by winds blowing generally from north and north-west. In contrast with the extreme
144 climatic condition, this region is known to be rich in ore deposits. The Antofagasta region hosts the main
145 Cu porphyry systems district of the world and most of the mines districts in the Taltal municipality are
146 from medium to large size exploitation and processing of Cu and Au ore deposits. Sadly, large amounts
147 of abandoned mine waste are found in the surroundings of Taltal city, discharged there after being
148 produced by Cu- and Au-related ores exploitation (CENMA, 2014). Mining activities have been carried
149 out for more than 100 years, attracting workers and producing an uncontrolled expansion of the urban
150 area, which ended up growing over and including abandoned mining wastes. Recent surveys have
151 allowed identifying and characterising the three largest abandoned mining wastes deposits of the Taltal
152 commune (S1, S2, and S3); one of them occurs within the Taltal city (S1), therefore posing risks of
153 direct and indirect exposure for the local communities. Compared to the S1, S2 and S3, S4 is of medium
154 size and is localised in the south-western part of the Taltal city. The geochemical composition of the
155 abandoned mining waste deposits is still unknown, and then their characterisation may be crucial to
156 prevent or control environmental pollution and human health risk to the local population.

157

158 **2.2. Sampling procedure and analyses**

159 A total of 125 topsoil samples was collected in the urban area of the Taltal city (6 km²) with an average
160 sampling density of approximately one sample per 0.05 km² (Fig. 2).

161

162 **[Figure 2 about here]**

163

164 The sampling procedure is based on the Geochemical Mapping of Agricultural and Grazing Land Soils
165 (GEMAS) sampling procedure described by Reimann et al. (2014). Each topsoil sample (from 0 to 20
166 cm ground top layer) was made by homogenizing 5 subsamples at the corners and the centre of a 100
167 m² square, collecting approximately 1.5 kg in total after removal of the impurities (stones, coarse
168 materials, and other debris). The soil samples were collected from the backyard of private houses,

169 parks, playgrounds and sidewalks of roads. At each sampling site the geographical coordinates system
170 were recorded by geospatial positioning systems (GPS). Containers used to collect samples were made
171 of high density polyethylene (Nalgene). Prior to their use, all of them were washed overnight with an
172 acid solution (HNO₃, 4 mol/L) and flushed with ultra-pure water. High purity chemicals and deionised
173 water were used to prepare all the solutions. All air-dried soil samples were sieved through a 2 mm
174 nylon sieve to remove some impurities (e.g. large stones) and finally stored in sealed polythene bags
175 prior to conduct physical and chemical analysis. The pH was measured in a 1:2.5 (w/v) soil-deionized
176 water suspension after 1 h long agitation (Pansu and Gautheyrou, 2006; Fuentes et al., 2014), with a
177 WTW multimeter (Proflin pH 3110 set 2 meter) equipped with a SenTix 41 pH electrode (Weilheim,
178 Germany). The electrical conductivity (EC) was determined in a saturation extract with a WTW Tetra
179 Con325 electrode and a Proflin Cond 3110 Set 1 meter (Weilheim, Germany). The redox potential (Eh)
180 was measured with a Pt–Ag/AgCl selective electrode on sample/deionized water suspensions at 1:2.5
181 ratio (w/v). The digestion of samples was performed by aqua regia extraction (ISO 11466) and
182 concentrations were determined according to EPA 6020A with an inductively coupled plasma optical
183 emission spectrometer (ICP-OES Agilent 5100, USA) in an accredited laboratory (ALS Life Sciences
184 Chile S.A) for 35 elements (Ag, Al, As, B, Ba, Be, Bi, Ca, Cd, Co, Cr, Cu, Fe, Ga, Hg, K, La, Mg, Mn,
185 Mo, Na, Ni, P, Pb, S, Sb, Sc, Sr, Th, Ti, Tl, U, V, W, and Zn). The calibration of equipment was
186 performed prior their use and reagent blanks were used for quality control. All the analytical results were
187 obtained as averages of three replicates. Precision of the analysis was calculated using three in-house
188 replicates, and two blind duplicates submitted by the authors. Accuracy was determined using ALS Life
189 Sciences Chile S.A's in-house reference material (Table 1).

190
191 [Table 1 about here]
192

193 **2.3. Geostatistical computations**

194 Two packages of the R software, “Compositions” (Van Den Boogaart et al., 2011) and
195 “Robcompositions” (Templ et al., 2011), were used for geostatistical computations. Univariate
196 descriptive statistic was computed (minimum, maximum, mean, median, Standard deviation, Coefficient
197 of Variation, kurtosis and skewness) using log-transformed data that was then back-transformed to
198 describe the central tendency and variability of the investigated elements. Although the log-ratio
199 transformation of data is more relevant in compositional data analysis, the summary statistics output
200 expressed in the raw concentrations of single elements is also meaningful and more easily interpretable
201 (Petrik et al., 2018a). A special emphasis was applied on 6 PTEs (As, Cd, Cr, Cu, Pb and Zn), trying to

202 identify the correlation between individual PTEs and the soil physicochemical properties (with pH, EC,
203 and potential redox) using Pearson correlation coefficients (r) and the p-values (with significance level of
204 $p < 0.05$).

205

206 **2.4. Geochemical mapping and robust factor analysis**

207 **2.4.1. Spatial distribution and baseline values of PTEs**

208 One of the main objectives of Geographical Information Systems (GIS) is to display spatial distribution
209 elements in studies areas through interpolation technics, further, shows their possible sources. Different
210 interpolated methods have been implemented to display spatial distribution of elements, reveal
211 geochemical processes, separating anomalies from background values as well the highlighting
212 elemental-sources patterns (Cheng et al., 1999; Lima et al., 2003; Luz et al., 2014). Conventional
213 weighted average technique such as kriging and ordinary inverse distance Weighted (IDW) smooth the
214 local variability of the geochemical data, whereas multifractal IDW creates a geochemical map in which
215 information about the local variability is retained (Cheng et al., 1999; Lima et al., 2003). Moreover,
216 Multifractal IDW interpolation preserves high frequency information, which is lost in any conventional
217 moving average methods such as kriging and ordinary inverse distance Weighted (IDW) (Cheng et al.,
218 1999). During interpolation and mapping of geochemical variables, both spatial association and scaling
219 are taken into account. More detailed description of MIDW method as well as Concentration-Area (C-A)
220 and Spectrum- Area (S-A) models and the state-of-art of these models have been clearly emphasized
221 by several authors (Cheng et al., 1999; Lima et al., 2003; Albanese et al., 2007; Petrik et al., 2018b).
222 For this study, one of the aims was to determine the spatial distribution of a group of PTEs (Cu, Zn, Pb,
223 As, Cr and Cd) and their respective baseline values in the soils of the Taltal city. ArcGIS (ESRI, 2012)
224 and GeoDAS (Cheng et al., 2001) software were used as the main GIS tools. In particular, GeoDAS™
225 provided interpolated geochemical maps by means of the multifractal inverse distance weighted (MIDW)
226 technique (Cheng et al., 1999; Lima et al., 2003; Thiombane et al., 2018a, 2018b). The C–A fractal
227 method (Cheng et al., 1994) that characterises image patterns and classifies them into components
228 based on a C-A plot, was applied to set the concentration intervals of the interpolated surfaces
229 generated by the MIDW method, and ArcGIS™ software was used for the graphical presentation of the
230 results.

231 Different studies have been conducted to determine background/baseline concentrations of elements
232 (Reimann et al., 2005; APAT-ISS, 2006; Tarvainen and Jarva, 2011; Cave et al., 2012; Ander et al.,
233 2013) and through this survey, we show showing baseline concentration ranges (where 'baseline'
234 indicates the actual content of an element in the superficial environment at a given point in time, as

235 defined by Salminen and Gregorauskiene (2000)) were obtained using the spectrum-areas method (S-A
236 plot), which preserves high frequency information (Cheng et al., 1999; Albanese et al.; 2007).
237 The S–A method is a fractal filtering technique, based on a Fourier spectral analysis (Cheng, 1999;
238 Cheng et al., 2001), and is used to separate anomalies from background values starting from a
239 geochemical interpolated concentrations map. It also uses both frequency and spatial information for
240 geochemical map and image processing. Fourier transformation can convert geochemical values into a
241 frequency domain in which different patterns of frequencies can be identified. The signals with certain
242 ranges of frequencies can be converted back to the spatial domain by inverse Fourier transformation
243 (Zuo et al., 2015; Zuo and Wang, 2016, Thiombane et al., 2019). The interpolated maps generated from
244 geochemical data were then transformed into the frequency domain in which a spatial concentration–
245 area fractal method was applied to distinguish the patterns on the basis of the power-spectrum
246 distribution. A log–log plot was used to show the relationship between the area and the power spectrum
247 values on the Fourier transformed map of the power spectrum. The values on the log–log plot were
248 modelled by fitting straight lines using least squares. Distinct classes can be generated, such as lower,
249 intermediate, and high power spectrum values approximately corresponding to baseline values,
250 anomalies, and noise of geochemical values in the spatial domain, respectively. The image, converted
251 back to a spatial domain with the filter applied, shows patterns that indicate an area that represents
252 baseline geochemical values of Cu, Zn, Pb, As, Cr, and Cd in our study area.

253

254 **2.4.2. Factor analysis**

255 Factor analysis (FA) is the multivariate statistical tool that explains the correlation structure of the
256 variables through a smaller number of factors (Reimann et al., 2002). In environmental geochemistry,
257 FA has been successfully used to reveal the elements sources related to their main hypothetical origins
258 (Albanese et al., 2007; Thiombane et al., 2018a). In this study, we have applied a robust FA and the
259 main procedures as well as the usefulness of this method has been highlighted in several publications
260 (Filzmoser et al., 2009a, Petrik et al., 2018b; Thiombane et al., 2018b). The different factors obtained
261 through the Robust FA were studied and interpreted in accordance with their presumed origin, i.e.
262 geogenic, anthropogenic or mixed (Reimann et al., 2002; Albanese et al., 2007).

263 The number of all measured elements (35) was reduced to 24 variables based on 2 main criteria: 1) the
264 removal of elements with more than 50% of observation values below the detection limit (DL), and 2)
265 choosing elements with a communality of extraction higher than 0.5 (50%) or common variances <0.5
266 (e.g. Reimann et al., 2002). As a consequence, both descriptive statistic and factor analysis were
267 performed on a reduced number of 24 variables.

299 The result range from 0 to 100% and highest grade of contamination is reflected by a RCCI value near
300 100%.

301

302 **3. Results and discussion**

303 **3.1. Spatial distribution and source patterns of PTEs**

304 Table 2 shows descriptive statistic of the 24 elements. Looking at skewness and kurtosis values, it can
305 be observed that variables are characterised by a right skewed distribution, except V (left-skewed).

306 **[Table 2 about here]**

307

308

309 This points out how raw data representation does not match well the “real” normal distribution mostly
310 due the presence of outliers. This is one of the main reasons why for further computations in this study,
311 all data were ilr-log transformed to express the normal data distribution, avoiding outliers’ artefacts and
312 spurious correlation (Egozcue et al., 2003; Filzmoser et al., 2009b; Hron et al., 2010). In terms of
313 variability, elements display large difference of CV values ranging from 36.20% (Al) to 398% (Mo). This
314 large CV values may be related to diversity of geological features and its physicochemical properties,
315 anthropogenic activities that could drive the distribution of these elements in soils of the study area.
316 Based on their spatial distribution, interrelationship as well as their harmful effect and adverse risk to
317 human health, a specific emphasis was given on a pool of 6 PTEs (As, Cd, Cr, Cu, Pb and Zn).

318 Figure 3 shows the spatial distribution of Cu, Zn, and Pb in soils of the Taltal city, with interpolated maps
319 interval ranges classified by using the concentration–area fractal method (C-A plot, plots below).

320

321 **[Figure 3 about here]**

322

323 Copper concentration values (Fig. 3A) range from 43 to 6,708 mg/kg in soils of Taltal city, with a mean
324 value of 766 mg/kg. The highest values (between 2,412 and 6,708 mg/kg) were found mostly in the
325 north-eastern part of the study area. This area corresponds also with one of the largest abandoned
326 mining waste deposits (S1) (see figure 2) of the Taltal municipality. Given the nature of the mining
327 activities, these Cu anomalies could be related to the presence of the specific mining waste deposit (S1)
328 which may affect concentrations in adjacent soils of the north-eastern part of our surveyed area.

329 Figures 3B and 3C present Pb and Zn values interpolated maps, ranging from 8.15 to 2,624 mg/kg with
330 a mean value of 135 mg/kg, and ranging from 45 to 2,241 mg/kg with a mean value of 224 mg/kg,
331 respectively. The lowest values of Pb (ranging from 8.15 to 42 mg/kg) and Zn (ranging from 45 to 153

332 mg/kg) are evident along the north-eastern part, corresponding to the inland external boundary of our
333 surveyed area. Values for these two elements gradually increase going towards the centre of the urban
334 area of Taltal city. These two elements can be related to anthropogenic activities such as industrial and
335 vehicular emission releases, which are characteristic of the urban areas. Similar results were also
336 described in Naples (Italy), being related to heavy traffic emission (Lima et al., 2003; Cicchella et al.,
337 2005; Petrik et al. 2018b). The highest values of Pb and Zn were found both in the north-eastern part of
338 our study area but in different locations. Similarly to Cu, high values of Pb and Zn were located in the
339 proximity of the abandoned mining waste deposit (S1); moreover, Pb displayed anomalous
340 concentration along the north-eastern part of the coastal side of our study area. The CENMA (2014) has
341 explained that the abandoned mining deposit (S1) in Taltal city “may be not only” made up of mine
342 tailing wastes, but also of possible metallurgical industrial waste dumps (e.g. batteries leaching waste).
343 Lead and Zn are essential materials in batteries (Linden, 1995) and anomalies of these two PTEs, in
344 Taltal city, may be related also to industrial wastes.

345 The interpolated map of As shows values ranging from 5.07 to 334.8 mg/kg with a mean value of 37.5
346 mg/kg (Fig. 4A).

347 **[Figure 4 about here]**

348

349 Arsenic displays anomalies in the south-western and north-eastern parts of the study area, where
350 values range from 81.56 to 334 mg/kg. It can be speculated that As patterns in Taltal city may be
351 influenced by anthropogenic activities, such as industrial waste and mining tailing abandoned in past
352 year. In fact, the south-western and north-eastern parts of the Taltal city are characterised by the
353 presence of mining waste deposits (S1 and S4), as already highlighted by CENMA (2014). The latter
354 might be indicated as the potential main sources of As in soils of our surveyed area. Figure 4B shows
355 the distribution of Cd, which presents high concentrations (ranging from 3.95 to 22.23 mg/kg) in the
356 north-eastern part of Taltal city, corresponding to the area where anomalous values of Cu, Zn, Pb, and
357 As are also found. On the other hand, spatial distribution of Cr, ranging from 2.09 to 85.8 mg/kg with a
358 mean value of 19.26 mg/kg presents a different spatial pattern compared to other PTEs (Cu, Pb, Zn, As
359 and Cd). The highest concentrations of Cr occur along the coast and south-western part of Taltal city,
360 where marine deposits prevail (sandstone and claystone) (Figs. 4C, 1B). In this case, anomalies of Cr
361 could be linked to geogenic enrichment of Cr in marine deposits of Taltal City. The Cr, being an “heavy”
362 element, resistant to alteration, would be enriched in marine sands as a “placer” concentrate (Kabata-
363 Pendias, 2011). Follow-up studies should be made to clarify better Cr higher concentrations in marine
364 deposits of the study area.

365 As a general observation, the mean concentration values of the 6 considered PTEs in soils of Taltal city
366 was compared with those in others urban areas from published studies (Table 3). Although the natural
367 (geological and climatic) characteristics are different among the various locations, these comparisons
368 usually allow for useful insight.

369

370

[Table 3 about here]

371

372 Tume et al. (2008) conducted a survey on soils of the Talcahuano city (central Chile), and their study
373 reported higher means values of Cr and Zn, compared to those found in Taltal city. A similar study
374 dealing with urban pollution, highlighted lower means values of As and Zn in soils of Sau Paulo (Brazil)
375 (Figueiredo et al., 2007). When compared to studies of larger Asian cities, it can be seen that the means
376 values of As, Cr, Cd, Cu, Pb and Zn in soils of Yibin city (China), Hong Kong (China) and Ulaanbaatar
377 (Mongolia) presented lower mean value compared to those of the present study. Similarly, comparisons
378 with studies conducted in three African cities, with the exception of Cd and Cr, values of the present
379 study all displayed higher concentrations (As, Cu, Pb, and Zn) compared to those of urban soils of
380 Ibadan (Nigeria), Annaba (Algeria) and Sfax (Tunisia). Even the large metropolitan area of Naples
381 (Southern Italy) showed lower means values of As, Cd, Cr, Cu, Pb, and Zn (Cicchella et al., 2005)
382 compared to those of the present study. On the other hand, soils in Glasgow (Scotland) (Ajmone-
383 Marsan et al., 2008) and Palermo (Italy) (Marta et al., 2002) displayed higher means values of Cr and
384 Pb, as well as Cd, Cr and Zn, compared to corresponding elements in soils of Taltal city. The only
385 element that consistently showed higher concentration values in the present study compared to those
386 carried out elsewhere is therefore Cu, which is consistent with the potential origin from abandoned
387 mining waste derived from Cu bearing deposit.

388

389

3.2. Correlation between PTEs and soils physicochemical properties

390 Values of redox potential, pH and (EC) ranged from 92.10 to 279 mV with a mean value of 183 mV,
391 from 6.86 to 9.89 with a mean 7.91, and 13 to 109,400 $\mu\text{S}/\text{cm}$ with a mean value of 12,550 $\mu\text{S}/\text{cm}$,
392 respectively (Table 2). A total of 93% of soils samples were classified as neutral to strongly alkaline.
393 Furthermore, based on their respective CV values, redox potential (CV= 19.75 mV) and pH (CV= 7.51)
394 displayed low variability in the studied soils.

395 Table 4 shows the linear correlation (based on Pearson correlation, r) and the significance of the
396 relationship between the 6 considered PTEs and the physicochemical properties of soils.

397 It was noticed that As and Pb present high positive correlation between them ($r = 0.69$) and with Cd
398 (with As, $r = 0.51$ and with Pb $r = 0.69$), Cu (with As, $r = 0.61$ and with Pb, $r = 0.61$) and Zn (with Pb, $r =$

399 0.48). This high correlation between the different PTEs points toward the same source, which in this
400 case is likely to be related to anthropogenic activities.

401

402

[Table 4 about here]

403

404 With the exception of Cr, it was noticed a negative high correlation ($r < - 0.45$) between the redox
405 potential and pH with As, Cd, Cu, Pb and Zn. This observation is consistent with acid pH and reducing
406 conditions where PTEs accumulate in soils. It is well known (e.g., Shuman, 1985; Violante et al. 2010)
407 that concentrations of metals(oids) can increase in soils that are characterised by acid pH and low
408 redox potential, which is mostly related to surface charge on oxides on Fe, Al and Mn or precipitation as
409 metal(loid) hydroxides (Stahl and James, 1991; Mouta et al., 2008). The mobility of elements such as
410 As, Cd, Cu, Pb and Zn in the studied soils seemed to be clearly correlated with physico-chemical
411 conditions. This was confirmed also by the p-values ($p < 0.05$), where significant correlations were
412 observed between redox potential and pH with all the 6 elements, whereas EC was correlated with As
413 and Cd.

414

415

3.3. Factor analysis and elements behaviour

416 The total variance of the 24 variables was 71.73% in the four-factor model, which was chosen based on
417 the break-point on the scree-plot of all factors. The 4 factors, named F1, F2, F3 and F4, account for
418 34.18%, 18.34%, 10.02% and 8.67% variability, respectively (Table 5).

419

420

[Table 5 about here]

421

422 Variables with loadings over the absolute value of 0.5 were considered to describe the main
423 composition of each factor. All variables hold communalities over 0.5 (50% of variability) meaning that
424 the 4 factor models capture fairly well the elemental interrelationships and their possible geogenic
425 and/or anthropogenic sources. The 24 elements of the four-factor model were separated by positive and
426 negative loadings and sorted in descending order:

427 F1= Pb, As, Sb, Ag, Cd, Cu, Mo, Ni, Zn, - (Mg, Al, Ti, Sc, K, Ca)

428 F2= Co, Fe, Mo, Ni, V, - (Ba, Sr, Ca, Na, K)

429 F3= Cr, V, Fe

430 F4= Mn, Be

431 The F1 association (Pb, As, Sb, Ag, Cd, Cu, Mo, Ni, Zn, - (Mg, Al, Ti, Sc, K, Ca)) accounts for the
432 highest total variance (34.18%) with good adequacy (eigenvalues = 9.15 > 1) between the factor and its

433 variables. Figure 5A shows the interpolated map of factor scores (F1), ranging from -1.73 to 2.96; high
434 factor scores (ranging from 1.43 to 2.96) were mapped in the north-eastern part of the Taltal city where
435 the abandoned mining waste deposit (S1) is found. This pool of elements is mostly made up of PTEs,
436 and their behaviour in soils of Taltal could be mostly related to an anthropogenic activity such as the
437 presence of the abandoned mining waste deposits (S1). Low factor scores (ranging from -1.73 to -0.48)
438 were found mostly in the eastern part of our study area, corresponding to an antithetic elemental
439 association including Mg, Al, Ti, Sc, K, and Ca. This association is likely to be related to a geogenic
440 source, and corresponds to an area where alluvial and colluvial deposits occur, made up by mixed
441 sedimentary and volcanic deposits underlined by calcareous sandstones (Escribano et al., 2013).

442

443 **[Figure 5 about here]**

444

445 The F2 association (Co, Fe, Mo, Ni, V, - (Ba, Sr, Ca, Na, K)) expressed 18.34% of the total variance
446 with an eigenvalue of 4.42, and factor scores ranging from -2.50 to 2.36. High factor scores values of F2
447 association (ranging from 1.34 to 2.36) were found in the north-eastern part of the study area (mostly
448 along the coast), in proximity of the S1 mining tailing deposit (Fig. 5B). A potential explanation for this
449 association is related to the accumulation of PTEs (Co, Ni, Mo, and V) linked with Fe hydroxides. In
450 oxidizing conditions, sorption and coprecipitation of hydrated cations such Co, Ni, Mo, and V is likely to
451 occur by adsorption onto Fe oxy-hydroxide (Koschinsky et al., 2003). In particular, the highest
452 concentrations of Fe (Fe > 202,254 mg/kg) were found in areas where this association actually displays
453 the highest factor scores values. The lowest factor scores loadings (from - 2.50 to - 0.37) were mostly
454 found in an area where occur marine, abrasion terrace deposits, and littoral cords deposits (Fig. 5B).
455 The antithetic elemental association (Ba, Sr, Ca, Na, and K) is likely to be related to geogenic source,
456 mostly pedogenic processes on abrasion terrace and littoral cords characterised by marine deposits,
457 conglomerate, and calcareous sandstone of the study area.

458 Figure 5C shows the interpolated map of factor scores (F3), ranging from -3.35 to 4.20, and it presents
459 the highest values (from 1.96 to 4.20) mostly in the coastal areas. These values could be related to
460 pedogenic processes in fine-size marine deposits, by sorption and coprecipitation of Cr and V with Fe
461 oxy-hydroxides in oxidizing environment (Stahl and James, 1991. Mouta et al., 2008); Cr and V
462 originating from ultrabasic rocks in the ocean may become “enriched” in marine sands similarly to a
463 “placer” concentrate. However, further studies are needed to better understand the source patterns of
464 Cr, which in this area displays particularly high concentrations.

465 The F4 association (Mn and Be) accounted a total variance of 8.67% with an eigenvalue of 1.39. The F4
466 factor score map (Fig. 5D) shows elevated values (ranging from 1.79 to 3.40), near the S1 abandoned

467 mining waste deposit, mostly in deposits of marine origin. Pedogenic processes inducing accumulation
468 of Mn and Be in this area could be linked to this association. Koschinsky et al. (2003) emphasized how
469 hydrated cations such as Be^{2+} have strong affinity with Mn-oxide in marine deposits.

470 In order to better distinguish and discriminate anthropogenic from geogenic sources of the considered 6
471 PTEs (As, Cd, Cr, Cu, Zn and Pb), a scatterplot of the covariate relationship between concentration
472 values with their respective distance to the abandoned mining waste deposit (S1) was employed (Fig.
473 6).

474

475 **[Figure 6 about here]**

476

477 In detail, figures 6A, 6b and 6C are scatter plots, showing the variation of Cd, Cu, As, Zn, Cr and Cd
478 concentrations values together with the distance of their corresponding sampling points from the
479 abandoned mining waste deposits (S1). The regression models of Cu, Pb, Zn, Cd and As concentration
480 values with their corresponding distance seem to follow a negative relationship, which is consistent with
481 a decrease of the concentrations of these PTEs with increasing distance from S1. Moreover, their
482 Pearson values confirm negative correlations between Cu ($r = -0.51$), Pb ($r = -0.38$), Zn ($r = -0.29$), Cd
483 ($r = -0.24$) and As ($r = -0.41$) and their corresponding distance from S1. This observation further indicates
484 how anomalies and patterns of Cu, Pb, Zn, Cd and As in soils of Taltal city are very likely to be driven by
485 the occurrence of abandoned mining waste deposit (S1).

486 On the other hand, the scatter plot between Cr concentration values and its corresponding distance to
487 S1 shows no correlation (no relationship, with $r = 0.03$) (Fig 6C). This observation precludes a link of
488 this element with the abandoned mining waste deposit, confirming that it is more probably related to
489 other mechanisms, such as Cr concentrations in marine sands.

490

491 **3.4. Baseline values of PTEs and Contamination level of Taltal city**

492 Figure 7 (plot below) presents results of the S-A fractal technique, which was used to determine the
493 spatial distribution of background/baseline values of Cu, Zn, Pb, As, Cr, and Cd in soils of the Taltal city,
494 and further distinguishes anthropogenic from geogenic contributions.

495

496 **[Figure 7 about here]**

497

498 Relatively low concentration values of Cu (ranging from 8.49 to 450 mg/kg) (Fig. 7), Zn (ranging from
499 4.18 to 260 mg/kg) (Fig. 8A), Pb (from 3.55 to 84.88 mg/kg) (Fig. 8B), As (from 1.22 to 39.32 mg/kg)
500 (Fig. 8C), Cd (ranging from 0.048 to 0.67) (Fig. 8D) and Cr (from 1.02 to 19.93 mg/kg) (Fig. 8E) were

501 found in most parts of Taltal city, and can be considered as the natural background variation for the
502 diverse lithologies that made up soils of the area. In contrast, higher baseline values Cu ($> 2,612$
503 mg/kg), Zn (> 608 mg/kg), Pb (from 428 to 926 mg/kg), Cd (from 3.08 to 6.78 mg/kg) were found in the
504 proximity of the abandoned mining waste deposit (S1). Fig. 8C shows high baseline values of As (from
505 105 to 162.4 mg/kg) in the north-eastern and south-western parts of Taltal city, where the S1 and S4
506 abandoned mining tailings deposits are located. Based on these observations, it can be speculated that
507 higher baseline values of Cu, Zn, Pb, Cd and As are related to the occurrence of abandoned mining
508 waste deposits in the proximity of (S4) and (S1). On the other hand, anomalous baselines values of Cr
509 shown along the coast confirm the interpretation that they could be related to pedogenic processes
510 affecting geogenic sources.

511

512

[Figure 8 about here]

513

514 In order to highlight the contamination level in soils of our study area, RCCI was computed for the 6
515 considered PTEs (As, Cd, Cr, Cu, Pb, and Pb).

516 Figure 9 presents the RCCI interpolated calculations, where lower values ($RCCI < 15\%$) were found in
517 the south and eastern parts of the study area, corresponding to a lower population density and no
518 industrial activities. This part of the city of Taltal seems therefore not affected by any contamination.

519

520

[Figure 9 about here]

521

522 Medium RCCI values (ranging from 15% to 25%) were found roughly in the inner and central parts of
523 the study area. This relatively low contamination may be related to small anthropogenic activities (e.g.
524 vehicular emission) that release additional quantities of the 6 considered PTEs in some areas of Taltal
525 city. However, in this area, anthropogenic releases of the 6 PTEs into environment are not significant.

526 Moderate (RCCI values ranging from 25 to 40%) and high (RCCI from 40 to 75%) contamination levels
527 were found in the north-eastern and south-western parts of the study area, characterised by an
528 abundance of elements such as As and Cr, and Cu and Pb, respectively. Based on these observations,
529 it can be established that high contamination levels are induced by two different anthropogenic inputs,
530 where the abandoned mining waste of the south-western part of the study area are Au-mining tailings
531 mostly rich in arsenopyrite (As) (S4), whilst the one in the north-eastern part is more closely linked to Cu
532 mining tailings (S1). A follow-up study would be necessary to better clarify the geochemical composition,
533 characterisation and possible identification of the specific type of mining wastes deposits (S1 and S4).

534 The highest values (RCCI > 75%) were found only in the north-eastern part (Cd>Pb>Cu) of the study
535 area. In particular, the predominance of Cd and Pb in soils confirms the findings of the CENMA (2014)
536 that highlighted this area as hosting industrial waste deposits (e.g. batteries leaching made up of Zn and
537 Pb alloys) in addition to mining tailings.

538

539 **4. Conclusion**

540 This study demonstrates with comprehensive mapping tools and geostatistical analysis, the source
541 patterns that drive multi-elements in soils of the study area, where robust computations have helped to
542 reveal the impact of abandoned industrial and mining waste deposits in soils of Taltal city, Chile.

543 Robust factor analysis, based on ilr-transformed data was performed to get an overview of elemental
544 associations and allowed to better distinguishing pool of elements related to the geological background
545 (e.g. Mg, Al, Ti, Sc, K, Ca, Ba, Sr, Ca, Na, K), pedogenic processes accompanying soil formation (Fe,
546 Mn, Cr, V, Be, Co, Mo, Ni, V) and anthropogenic activities (e.g. Pb, As, Sb, Ag, Cd, Cu, Mo, Ni, Zn).
547 Mapping tools (Fractal methods) allowed displaying spatial distribution of the considered 6 PTEs and
548 the behaviours of As, Cd, Cu, Pb and Zn, associated with the presence of abandoned waste mining
549 deposits as well as with the physicochemical conditions of soils. Chromium was associated to
550 pedogenic processes of sorption and coprecipitation in fine-size deposits of marine origin. Low baseline
551 values of PTEs were found in most of the survey area and high values were often very small in extent,
552 except for some sites where the anthropogenic influence on soils is clearly evident, due to the potential
553 influence of extensive abandoned mining waste deposits (e.g., north-eastern part of the Taltal city). The
554 integrated approach used in this study allowed a more robust qualitative and quantitative evaluation of
555 contamination level, highlighting very high contamination levels, where the findings from the various
556 tools converge all in the same direction, pointing out a strong link with abandoned mining tailings and
557 industrial waste deposits. Results from this study strongly suggest that a more detailed and thorough
558 assessment of PTEs should be conducted for a comprehensive evaluation of human health risk due to
559 PTEs exposure.

560

561 **Acknowledgements**

562 We appreciate the contribution (Software support) from Annalise Guarino, PhD student from the
563 Department of Earth Sciences, Environment and Resources (DISTAR), University of Naples, "Federico
564 II". This work was supported through two financial supports: 1) *Funding from the Regional Council of*
565 *Antofagasta under Project "Estudio de ingeniería para la remediación de sitios abandonados con*
566 *potencial presencia de contaminantes identificados en la comuna de Taltal - BIP N°30320122-0" and by*

567 2) "Conicyt + Fondef/ Tercer Concurso Idea en dos etapas del fondo de fomento al desarrollo científico
568 y tecnológico. Fondef/Conicyt 2016+ Folio (Código IT16M10031), Mapa de la línea base geoquímica
569 para suelos en la comuna de Taltal: LIBAMET–Map Services".

570

571

572 **References**

573 Aitchison, J., Egozcue, J., 2005. Compositional data analysis: where are we and where should we be
574 heading? *Math. Geol.* 37, 829–850.

575 Albanese, S., De Vivo, B., Lima, A., Cicchella, D., 2007. Geochemical background and baseline values
576 of toxic elements in stream sediments of Campania region (Italy). *J. Geochem. Explor.* 93 (1), 21–34.

577 Albanese, S., De Vivo, B., Lima, A., Cicchella, D., Civitillo, D., Cosenza, A., 2010. Geochemical
578 baselines and risk assessment of the Bagnoli brownfield site coastal sea sediments (Naples, Italy). *J.*
579 *Geochem. Explor.* 105, 19–33.

580 Ander, E.L., Johnson, C.C., Cave, M.R., Palumbo-Roe, B., Nathanail, C.P., Lark, R.M., 2013.
581 Methodology for the determination of normal background concentrations of contaminants in English soil.
582 *Sci. Total Environ.* 454–455, 604–618.

583 APAT-ISS, 2006. Protocollo Operativo per la determinazione dei valori di fondo di metalli/ metalloidi nei
584 suoli dei siti d'interesse nazionale. Revisione 0. Agenzia per la Protezione dell'Ambiente e per i Servizi
585 Tecnici and Istituto Superiore di Sanita (in Italian).

586 Azevedo-Silva, C.E., Almeida, R., Carvalho, D.P., Ometto, J.P.H.B., de Camargo P.B., Dorneles, P.R.,
587 Azeredo, Antonio, Wanderley, R.B., Olaf, M., Torres, J.P.M., 2016. Mercury biomagnification and the
588 trophic structure of the ichthyofauna from a remote lake in the Brazilian Amazon. *Environ. Res.* 151, 286-
589 296.

590 Batjargal, T., Otgonjargal, E., Baek, K., Yang, J.S., 2010. Assessment of metals contamination of soils
591 in Ulaanbaatar, Mongolia. *J. Hazard. Mater* 184, 872-876.

592 Biasioli, M., Grčman, H., Kralj, T., Madrid, F., Diaz-Barrientos, E., Ajmone-Marsan, F., 2007. Potentially
593 toxic elements contamination in urban soils: a comparison of three European cities. *J. Environ. Qual.* 36,
594 70–79.

595 Bundschuh, J., Litter, M.I., Parvez, F., Román-Ross, G., Nicolli, H.B., Jean, J.-S., Liu, C.-W., López, D.,
596 Armienta, M.A., Guilherme, L.R.G., Cuevas, A.G., Comejo, L., Cumbal, L., Toujaguez, R. 2012. One
597 century of arsenic exposure in Latin America: a review of history and occurrence from 14 countries. *The*
598 *Science of the Total Environment*, 429: 2–35. [https:// doi.org/10.1016/j.scitotenv.2011.06.024](https://doi.org/10.1016/j.scitotenv.2011.06.024).

599 Cave, M.R., Johnson, C.C., Ander, E.L., Palumbo-Roe, B., 2012. Methodology for the determination of
600 normal background contaminant concentrations in English soils. In: British Geological Survey
601 Commissioned Report, CR/12/003, (41 pp.). <http://nora.nerc.ac.uk/19959/>.

602 CENMA. 2014. Informe final Versión 5. Diagnostico regional de suelos abandonados con potencial
603 presencia de contaminantes. Contrato N° 618775-3-LP13. [Spanish]

604 Cheng, Q., 1999. Spatial and scaling modelling for geochemical anomaly separation. *J. Geochem.*
605 *Explor.* 65, 175–194.

606 Cheng, Q., Agterberg, F.P., Ballantyne, S.B., 1994. The separation of geochemical anomalies from
607 background by fractal methods. *J. Geochem. Explor.* 51, 109–130.

608 Cheng, Q., Bonham-Carter, G.F., Raines, G.L., 2001. GeoDAS: a new GIS system for spatial analysis
609 of geochemical data sets for mineral exploration and environmental assessment. In: *The 20th Intern.*
610 *Geochem. Explor. Symposium (IGES)*. Santiago de Chile. Vol. 6/5–10/5. pp. 42–43.

611 Chester, R., Stoner, J.H., 1973. Pb in particulates from the lower atmosphere of the eastern Atlantic.
612 *Nature* 245, 27–28.

613 Cicchella, D., De Vivo, B., Lima, A., 2005. Background and baseline concentration values of elements
614 harmful to human health in the volcanic soils of the metropolitan and provincial area of Napoli (Italy).
615 *Geochem. Explor. Environ. Anal.* 5, 29–40.

616 Comas-Cufí, M., Thió-Henestrosa, S., 2011. CoDaPack 2.0: a stand-alone, multi-platform compositional
617 software. In: Egozcue, J.J., Tolosana-Delgado, R., Ortego, M.I. (Eds.), *CoDaWork'11: 4th International*
618 *Workshop on Compositional Data Analysis*. SantFeliu de Guíxols.

619 Egozcue, J.J., Pawlowsky-Glahn, V., Mateu-figueras, G., Barcelo-vidal, C., 2003. Isometric logratio
620 transformations for compositional data analysis. *Math. Geol.* 35 (3), 279–300.

621 Escribano, J., Martínez, P., Domagala, J., Padel, M., Espinoza, M., Jorquera, R.,...Calderón, M.
622 (2013). *Cartas Bahía Isla Blanca y Taltal*. Escala 1:100.000. Servicio Nacional de Geología y
623 Minería, *Carta Geológica de Chile, Serie Geología Básica*, 164-165. 1–75. 1 mapa escala 1:100.000.
624 Santiago.[Spanish].

625 ESRI (Environmental Systems Research Institute), 2012. *ArcGIS Desktop: Release 10*. Redlands, CA.

626 Ezeigbo Hl., Ezeanyim BN. (1993). Environmental pollution from coal mining activities in the Enugu
627 Area, Anambra State, Nigeria. *Mine Water Environ.*, 12: 53-62.

628 Figueiredo, A.M.G., Nogueira, C.A., Saiki, M., Milian, F.M., Domingos, M., 2007. Assessment of
629 atmospheric metallic pollution in the metropolitan region of São Paulo, Brazil. *Environ. Pollut.*
630 145,279–292.

631 Filzmoser, P., Hron, K., Reimann, C., 2009a. Principal component analysis for compositional data with
632 outliers. *Environmetrics* 20 (6), 621–632.

633 Filzmoser, P., Hron, K., Reimann, C., 2009b. Univariate statistical analysis of environmental
634 (compositional) data - problems and possibilities. *Sci. Total Environ.* 407, 6100–6108.

635 Guillén, M.T., Delgado, J., Albanese, S., Nieto, J.M., Lima, A., De Vivo, B., 2011. Environmental
636 geochemical mapping of Huelva municipality soils (SW Spain) as a tool to determine background and
637 baseline values. *J. Geochem. Explor.* 109 (1–3), 59–69. <https://doi.org/10.1016/j.gexplo.2011.03.003>.

638 Guo, G.H., Wu, F.C., Xie, F.Z. & Zhang, R.Q. 2012. Spatial distribution and pollution assessment of
639 heavy metals in urban soils from southwest China. *Journal of Environmental Sciences*,24,410–418.

640 Hakanson, L., 1980. An ecological risk index for aquatic pollution control. A sedimentological approach.
641 *Water Res.* 14 (8), 975–1001, [https://doi.org/10.1016/0043-1354\(80\)90143-8](https://doi.org/10.1016/0043-1354(80)90143-8).

642 Han, J., Kamber, M., 2001. *Data Mining: Concepts and Techniques*. Morgan-Kaufmann Academic
643 Press, San Francisco.

644 Hron, K., Templ, M., Filzmoser, P., 2010. Imputation of missing values for compositional data using
645 classical and robust methods. *Comput. Stat. Data Anal.* 54 (12), 3095–3107.

646 ISO 11466. ISO. Soil Quality. Extraction of Trace Elements Soluble in Aqua Regia. ISO 11466. 1995.

647 Jmone-Marsan, F., Biasioli, M., Kralj, T., Grčman, H., Davidson, C.M., Hursthouse, A.S., Madrid, L.,
648 Rodrigues, S., 2007. Metals in particle-size fractions of the soils of five European cities. *Environ. Pollut.*
649 152, 73–81.

650 Kabata-Pendias, A., 2011. *Trace Elements of Soils and Plants*, fourth ed. CRC Press, Taylor & Francis
651 Group, LLC, USA, pp. 28–534.

652 Koschinsky A, Winkler A, Fritsche U. Importance of different types of marine particles for the scavenging
653 of heavy metals in the deep-sea bottom water. *Applied Geochemistry.* 2003;18 (5):693-710

654 Li, X., Lee, S.L., Wong, S.C., Shi, W., Thornton, I., 2004. The study of metal contamination in urban
655 soils of Hong Kong using a GIS-based approach. *Environmental Pollution* 129, 113–124.

656 Linden, D. *Handbook of Batteries*, McGraw-Hill, New York, 1995, pp. 32.1–32.11.

657 Lim, H.S., Lee, J.S., Chon, H.T., Sager, M., 2008. Heavy metal contamination and health risk
658 assessment in the vicinity of the abandoned Songcheon Au–Ag mine in Korea. *J. Geochem. Explor.* 96
659 (2–3), 223–230. <https://doi.org/10.1016/j.gexplo.2007.04.008>.

660 Lima, A., De Vivo, B., Cicchella, D., Cortini, M., Albanese, S., 2003. Multifractal IDW interpolation and
661 fractal filtering method in environmental studies: an application on regional stream sediments of
662 Campania Region (Italy). *Appl. Geochem.* 18 (12), 1853–1865.
663 [https://doi.org/10.1016/S08832927\(03\)00083-0](https://doi.org/10.1016/S08832927(03)00083-0).

664 Luo, X.S., Yu, S., Zhu, Y.G., Li, X.D., 2011. Trace metal contamination in urban soils of China. *Science
665 of the Total Environment* 421-422, 17-30.

666 Luo, Y., Wu, L., Liu, L., Han, C. Li, Z. 2009. Heavy Metal Contamination and Remediation in Asian
667 Agricultural Land. p. 9. Paper presented at MARCO Symposium, 2009, Japan.

668 Luz, F., Mateus, A., Matos, J.X., Gonçalves, M.A., 2014. Cu-and Zn-soil anomalies in the NE Border of
669 the South Portuguese Zone (Iberian Variscides, Portugal) identified by multifractal and geostatistical
670 analyses. *Natural Resources Research* 23, 195-215

671 Maas, S., Scheifler, R., Benslama, M., Crini, N., Lucot, E., Brahmia, Z., Benyacoub, S., Giraudoux, P.
672 2010. Spatial distribution of heavy metal concentrations in urban, suburban and agricultural soils in a
673 Mediterranean city of Algeria, *Environmental Pollution* 158(6):2294-2301.

674 Manta, D.S., Angelone, M., Bellanca, A., Neri, R., Sprovieri, M., 2002. Heavy metals in urban soils: a
675 case study from the city of Palermo (Sicily), Italy. *Sci. Total Environ.* 300, 229–243.

676 Mouta, E.R. Soares, M.R., Casagrande, J.C. 2008. Copper adsorption as a function of solution
677 parameters of variable charge soils. *J. Braz. Chem. Soc.* 19, 996-1009.

678 Müller, G., 1969. Index of Geoaccumulation in sediments of the rhine river. *Geo Journal* 2, 108-118.

679 Müller, G., 1981. The heavy metal pollution of the sediments of Neckars and its tributary: a stock taking.
680 *Chem. Ztg.* 105, 157–164.

681 Naicker K, Cukrowska E, McCarthy TS (2003). Acid mine drainage from gold mining activities in
682 Johannesburg, South Africa and environs. *Environ. Pollut.*, 122: 29-40.

683 Odewande, A.A., and A.F. Abimbola. 2008. Contamination indices and heavy metal concentrations in
684 urban soil of Ibadan metropolis, southwestern Nigeria. *Environ. Geochem. Health* 30:243–254.

685 Pawlowsky-Glahn, V., Buccianti, A., 2011. *Compositional Data Analysis: Theory and Applications*. John
686 Wiley Sons.

687 Pawlowsky-Glahn, V., Egozcue, J.J., Tolosana-Delgado, R., 2015b. *Modelling and Analysis of*
688 *Compositional Data*. John Wiley Sons, pp. 252.

689 Petrik, A., Thiombane, M., Lima, A., Albanese, S., Buscher, J.T., De Vivo, B. 2018a. Soil contamination
690 compositional index: A new approach to quantify contamination demonstrated by assessing
691 compositional source patterns of potentially toxic elements in the Campania Region (Italy). *Applied*
692 *Geochemistry*. 96, 264-276.

693 Petrik, A., Thiombane, M., Albanese, S., Lima, A., De Vivo, B., 2018b. Source patterns of Zn, Pb, Cr
694 and Ni potentially toxic elements (PTEs) through a compositional discrimination analysis: a case study
695 on the Campanian topsoil data. *Geoderma*. 331, 87–99.

696 Prapamontol, T., Stevenson, D. 1991. Rapid method for the determination of organochlorine pesticides
697 in milk. *J. Chromatogr.* 552, 249-257.

698 Reimann, C., Birke, M., Demetriades, A., Filzmoser, P., O'Connor, P., GEMAS Team, 2014. Chemistry
699 of Europe's agricultural soils — part A: methodology and interpretation of the GEMAS data set. In:
700 *Geologisches Jahrbuch (Reihe B)*. Schweizerbarth, Hannover, pp. 528.

701 Reimann, C., de Caritat, P., 2000. Intrinsic flaws of element enrichment factors (EFs) in environmental
702 geochemistry. *Environ. Sci. Technol.* 34, 5084–5091.

703 Reimann, C., Filzmoser, P., Garrett, R., 2002. Factor analysis applied to regional geochemical data:
704 problems and possibilities. *Appl. Geochem.* 17 (3), 185–206.

705 Reimann, C., Filzmoser, P., Garrett, R.G., Dutter, R., 2008. Statistical data analysis explained. In:
706 *Applied Environmental Statistics with R*. Wiley, Chichester, pp. 362. Chemistry of Europe's agricultural
707 soils — part A: methodology and interpretation of the GEMAS data set. In: Reimann, C., Birke, M.,
708 Demetriades, A., Filzmoser, P., O'Connor, P., GEMAS Team (Eds.), *Geologisches Jahrbuch (Reihe B)*,
709 Schweizerbarth: Hannover, pp. 528.

710 Reimann, C., Garrett, R.G., 2005. Geochemical background – concept and reality. *Sci. Total Environ.*
711 350, 12–27.

712 Salminen, R., Gregorauskiene, V., 2000. Considerations regarding the definition of a geochemical
713 baseline of elements in the surficial materials in areas differing in basic geology. *Appl. Geochem.* 15,
714 647–653.

715 Shuman, L.M. 1985. Effect of ionic strength and anions on zinc adsorption by two soils. *Soil Sci. Soc.*
716 *Am. J.* 50, 1438-1442.

717 Stahl, R.S., James, B.R. 1991. Zinc sorption by B horizon soils as a function of pH. *Soil Sci. Soc. Of*
718 *Am. J.* 55, 1592-1597.

719 Suchan, P., Pulkrabová, J., Hajslová, J., Kocourek, V., (2004). Pressurized liquid extraction in
720 determination of polychlorinated biphenyls and organochlorine pesticides in fish samples. *Anal. Chim.*
721 *Acta.* 520,193–200.

722 Sucharovà, J., Suchara, I., Hola, M., Marikova, S., Reimann, C., Boyd, R., Filzmoser, P., Englmaier, P.,
723 2012. Top-/Bottom-soil ratios and enrichment factors: what do they really show? *Appl. Geochem.* 27,
724 138–145.

725 Tarvainen, T., Jarva, J., Johnson, C.C., Ottesen, R.T., 2011. Using geochemical baselines in the
726 assessment of soil contamination in Finland. In: Demetriades, A., Locutura, J. (Eds.), *Mapping the*
727 *Chemical Environment of Urban Areas*. Chichester, UK, John Wiley Sons Ltd., pp. 223–231.

728 Templ, M., Hron, K., Filzmoser, P., 2011. *Rob-Compositions: Robust Estimation for Compositional Data.*
729 *Manual and Package, Version 1.4.4.*

730 Thiombane, M., Martin-Fernandez, J.A., Albanese, S., Lima, A., Doherti, A., De Vivo, B., 2018a.
731 Exploratory analysis of multi-element geochemical patterns in soil from the Sarno River Basin
732 (Campania region, southern Italy) through compositional data analysis (CODA). *J. Geochem. Explor.*
733 195, 110-120.

734 Thiombane, M., Zuzolo, D., Cicchella, D., Albanese, S., Lima, A., Cavaliere, M., De Vivo, B., 2018b. Soil
735 geochemical follow-up in the Cilento World Heritage Park (Campania, Italy) through exploratory
736 compositional data analysis and C-A fractal model. *J. Geochem. Explor.* 189, 85–99.

- 737 Thiombane, M., Di Bonito, M., Albanese, A., Zuzolo, D., Lima, A., De Vivo, D. 2019. Geogenic versus
738 anthropogenic behaviour of geochemical phosphorus footprint in the Campania region (Southern Italy)
739 soils through compositional data analysis and enrichment factor. *Geoderma*. 335, 12-26.
- 740 Tume, P., J. Bech, B. Sepulveda, L. Tume, and J. Bech. 2008. Concentrations of heavy metals in urban
741 soils of Talcahuano (Chile): A preliminary study. *Environ. Monit. Assess.* 140:91–98.
- 742 Van Den Boogaart, K.G., Tolosana-Delgado, R., Bren, R., 2011. Compositions: Compositional Data
743 Analysis. R Package Version 1. pp. 10–12. Available at:
744 <http://CRAN.Rproject.org/package=compositions>.
- 745 Violante, A., Cozzolino, V., Perelomov, L., Caporale, A., Pigna, M. 2010. Mobility and bioavailability of
746 heavy metals and metalloids in soil environments *J. Soil Sci. Plant Nutr.* 10, 268-292.
- 747 Wali, A., Colinet, G., Khadhraoui, M. Ksibi, M. 2013. Trace Metals in Surface Soil Contaminated by
748 Release of Phosphate Industry in the Surroundings of Sfax-Tunisia. *Environmental research,*
749 *engineering and management.* Vol 65, No 3 <http://dx.doi.org/10.5755/j01.arem.65.3.4865>.
- 750 Wang, Y., Sikora, S., Kim, H., Dubey, B., Townsend, T., 2012. Mobilization of iron and arsenic from soil
751 by construction and demolition debris landfill leachate. *Waste Manag.* 32 (5), 925–932.
752 <https://doi.org/10.1016/j.wasman.2011.11.016>.
- 753 Wu, S., Peng, S., Zhang, X., Wu, D., Luo, W., Zhang, T., Zhou, S., Yang, G., Wan, H., Wu, L., 2015.
754 Levels and health risk assessments of heavy metals in urban soils in Dongguan, China. *J. Geochem.*
755 *Explor.* 148, 71–78. <https://doi.org/10.1016/j.gexplo.2014.08.009>.
- 756 Zuo, R., Wang, J., 2016. Fractal/multifractal modelling of geochemical data: a review. *J. Geochem.*
757 *Explor.* 164, 33–41. Zuo, R., Wang, J., Chen, G., Yang, M., 2015. Identification of weak anomalies: a
758 multifractal perspective. *J. Geochem. Explor.* 148, 12–24.
- 759 Zuo, R., Wang, J., Chen, G., Yang, M., 2015. Identification of weak anomalies: a multifractal
760 perspective. *J. Geochem. Explor.* 148, 12–24.

761

762 **Figure and table captions**

763 **• Figures**

764 **Figure 1.** Geo-localisation of the Taltal city (Fig. 1A), main geological features (Fig. 1B) and Landuse
765 (Fig. 1C) of the surveyed area

766 **Figure 2.** Sampling points and location of the abandoned mining waste deposits (S1, S2, S3 and S4) in
767 (around) the study area

768 **Figure 3.** Interpolated maps of Cu, Zn, and Pb concentrations values in the survey area; ranges of
769 concentration are based on the C-A fractal plots held bellow

770 **Figure 4.** Interpolated maps of As, Cr, and Cd concentrations values in the survey area; ranges of
771 concentration are based on the C-A fractal plots held bellow

772 **Figure 5.** Interpolated factor score map of the factor 1 (F1, 5A), factor 2 (F2, 5B), factor 3 (F3, 5C) and
773 factor 4 (F4, 5D). Factor score values ranges are created by means of fractal concentration–area plot
774 (C–A method)

775 **Figure 6.** Scatterplots between concentration values of Cu, Pb, Zn, As, Cr and Cd (PTEs) with distance
776 from abandoned mining waste deposit (S1); (r) symbolizes Pearson correlation values that highlight the
777 covariate relationship between two variables.

778 **Figure 7.** Interpolated baseline map of Cu soils of Taltal city; the plot bellow symbolises Spectrum-Area
779 (S-A) plot for Cu data: the vertical axis represents $\log A(\geq E)$ and the horizontal axis the log-transformed
780 power spectrum value itself; the cut-off indicated by the vertical line was applied to generate the
781 corresponding filter used for geochemical baseline map.

782 **Figure 8.** Interpolated baseline maps of Zn (8A), Pb (8B), As (8C), Cd (8D) and Cr (8E) concentrations
783 values in soils of our study area

784 **Figure 9.** RCCI interpolated and dots map of the 6 considered PTEs; values are expressed in
785 percentage (%) and red colour symbolises very high contamination level

786

787 • Tables

788 **Table 1.** Detection limit, accuracy and precision of the applied analytical method (RPD =relative
789 percent difference). The Precision was calculated as relative percentage difference (%RPD) using the
790 formula: $\%RPD = \frac{|SV - DV|}{SV + DV} \times 100$, where SV =the original sample value, DV=the
791 duplicate sample value. The laboratory accuracy error was determined using the formula: Accuracy
792 error= $\frac{|X - TV|}{TV} \times 100$, where X =laboratory's analysis result for the performance sample (standard)
793 and TV= true value of the performance sample (standard)

794 **Table 2.** Descriptive statistic of 125 topsoils samples from the Taltal urban area, Northern Chile; CV and
795 Std. Deviation are the coefficient of variation (%) and standard deviation, respectively

796 **Table 3.** Mean concentrations values of 6 considered PTES (mg/kg) in topsoil of the survey area
797 compared to values found in other studies in the recent literature

798 **Table 4.** Linear correlation (based on Pearson correlation, r values in black) and the significance of the
799 relationship (p-values <0.05, symbolised in red colour) between six PTEs and with the physicochemical
800 properties (pH, EC and redox potential) in soils of Taltal city

801 **Table 5.** Varimax-rotated factor (four-factor model) of isometric log-ratio ilr back-transformed variables
802 for 125 topsoil samples from the survey area; bold entries: loading values over |0.50|

Figure 1.

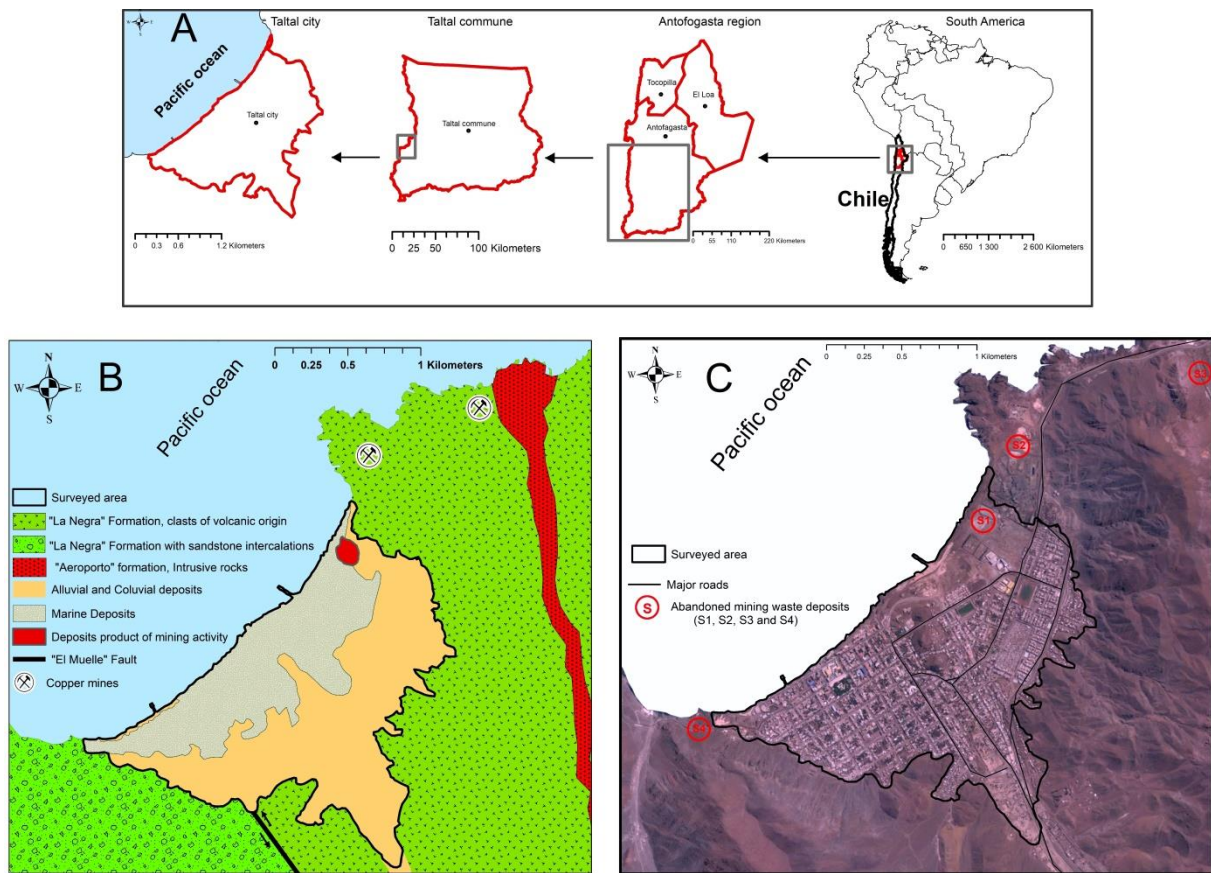


Figure 2.

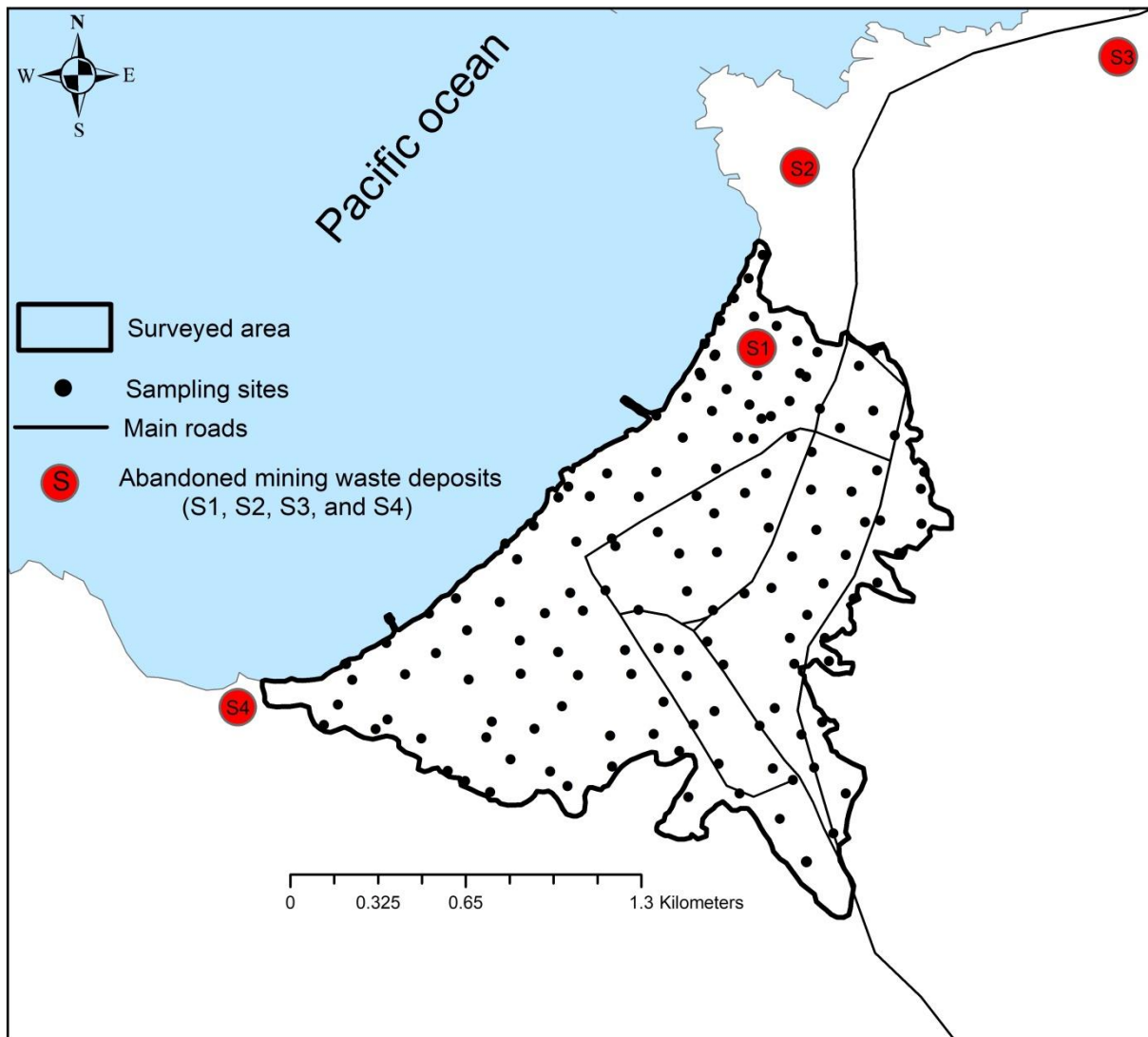


Figure 3.

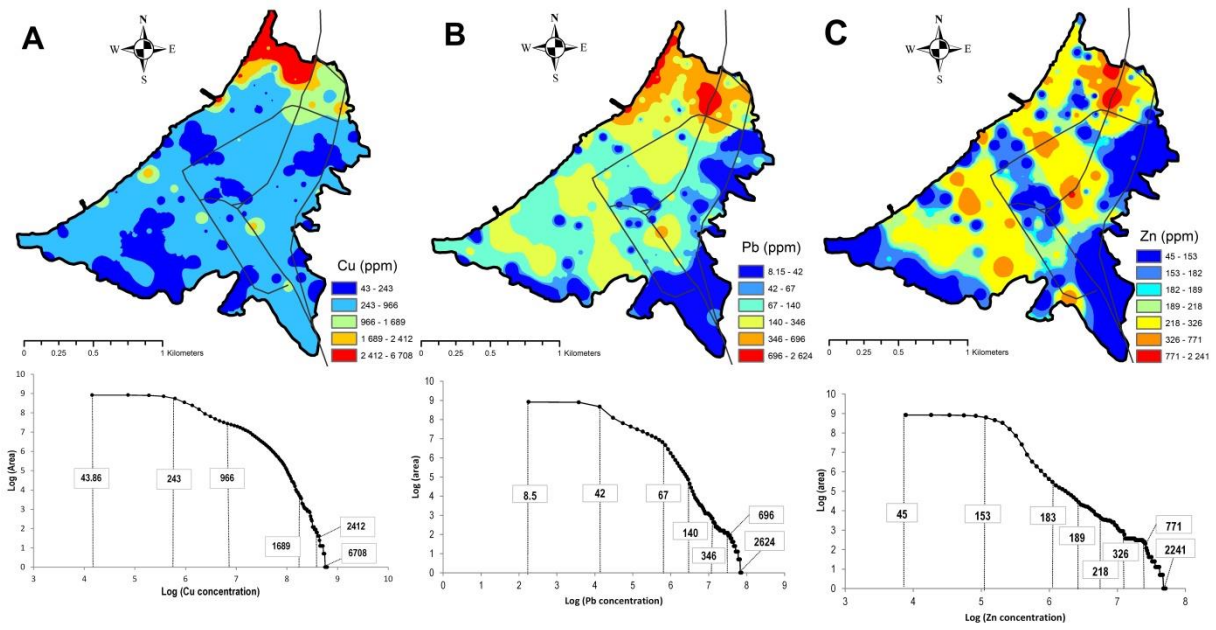


Figure 4.

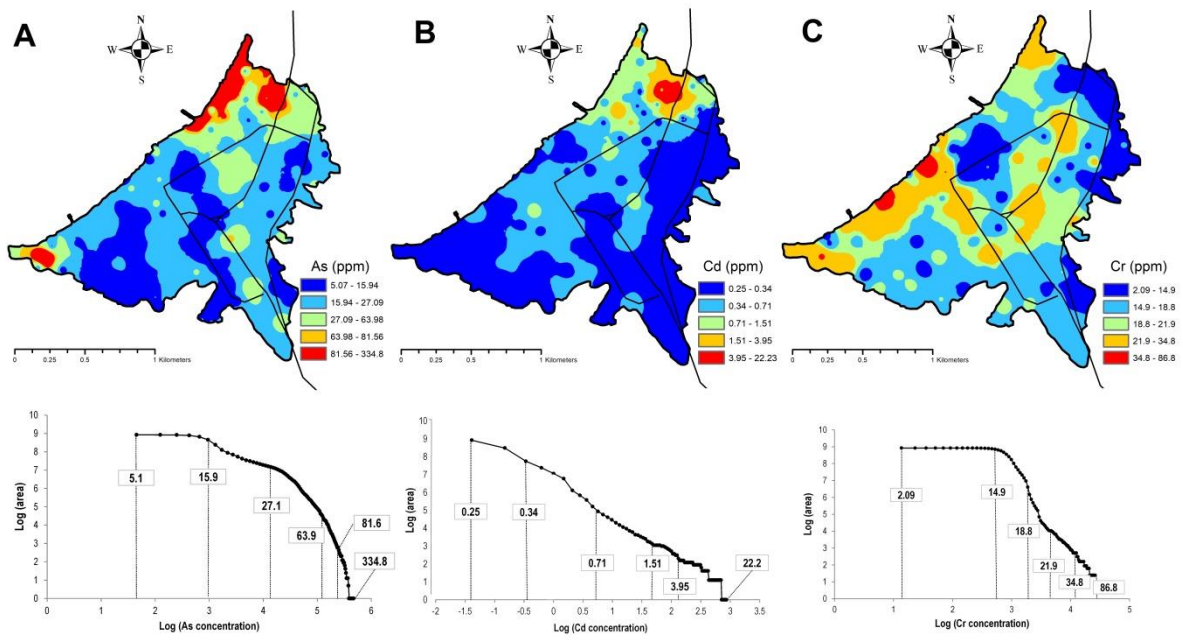
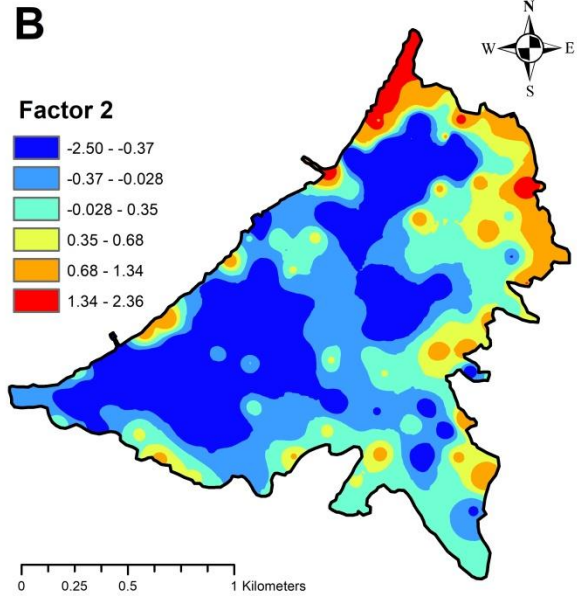
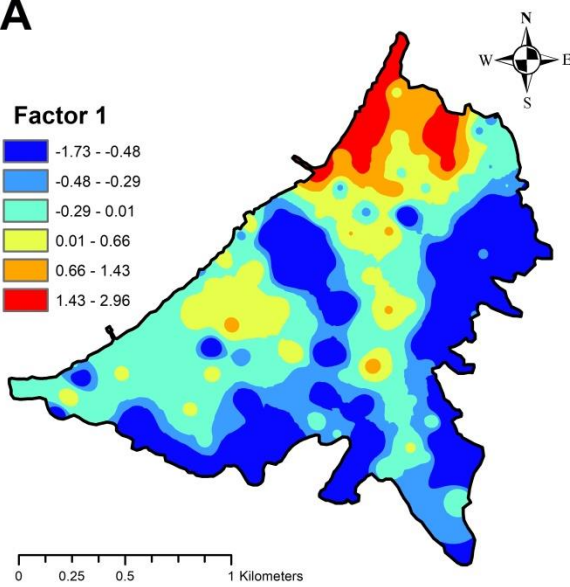
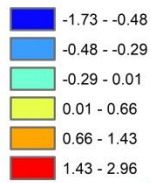


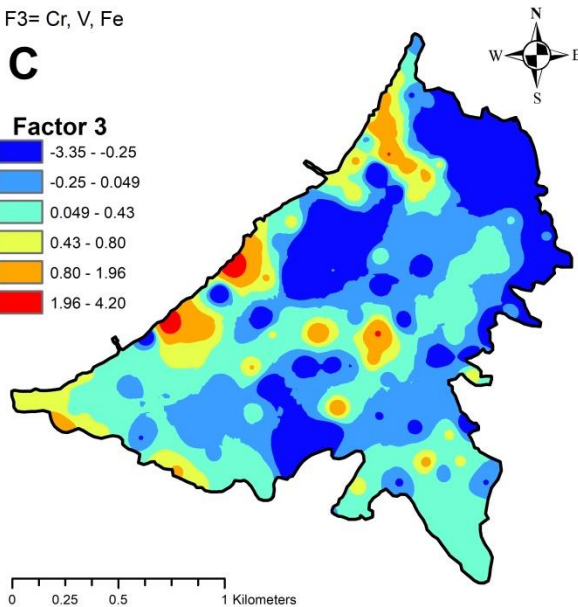
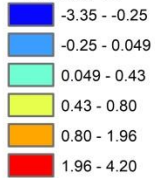
Figure 5.

F1= (Pb, As, Sb, Ag, Cd, Cu, Mo, Ni, Zn), - (Mg, Al, Ti, Sc, K, Ca)

F2= (Co, Fe, Mo, Ni, V), - (Ba, Sr, Ca, Na, K)

A**Factor 1**

F3= Cr, V, Fe

C**Factor 3**

F4= Mn, Be

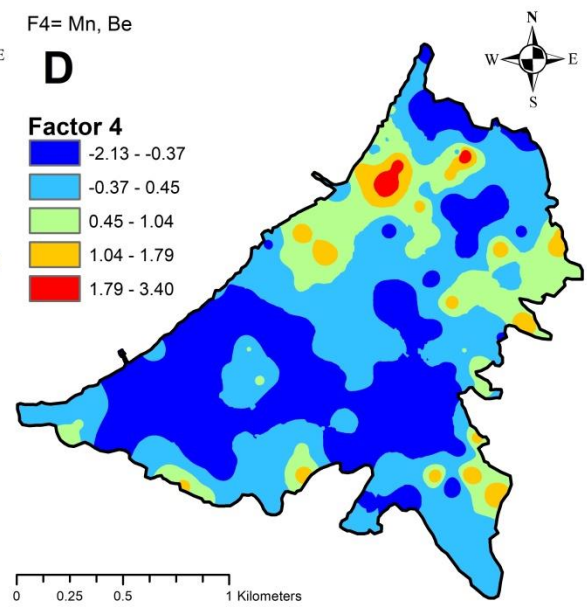
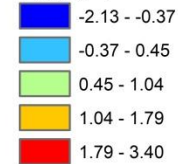
D**Factor 4**

Figure 6.

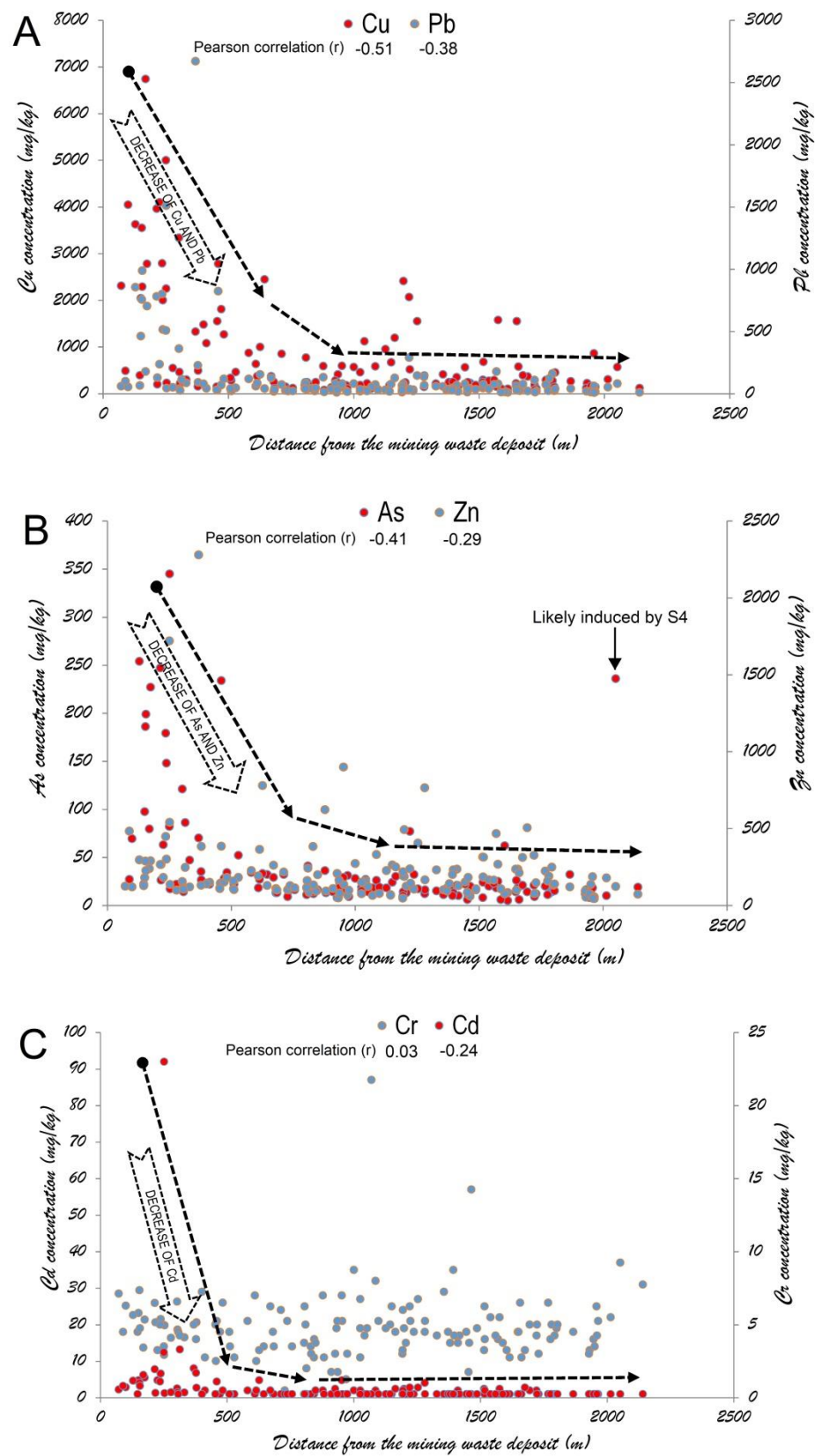


Figure 7.

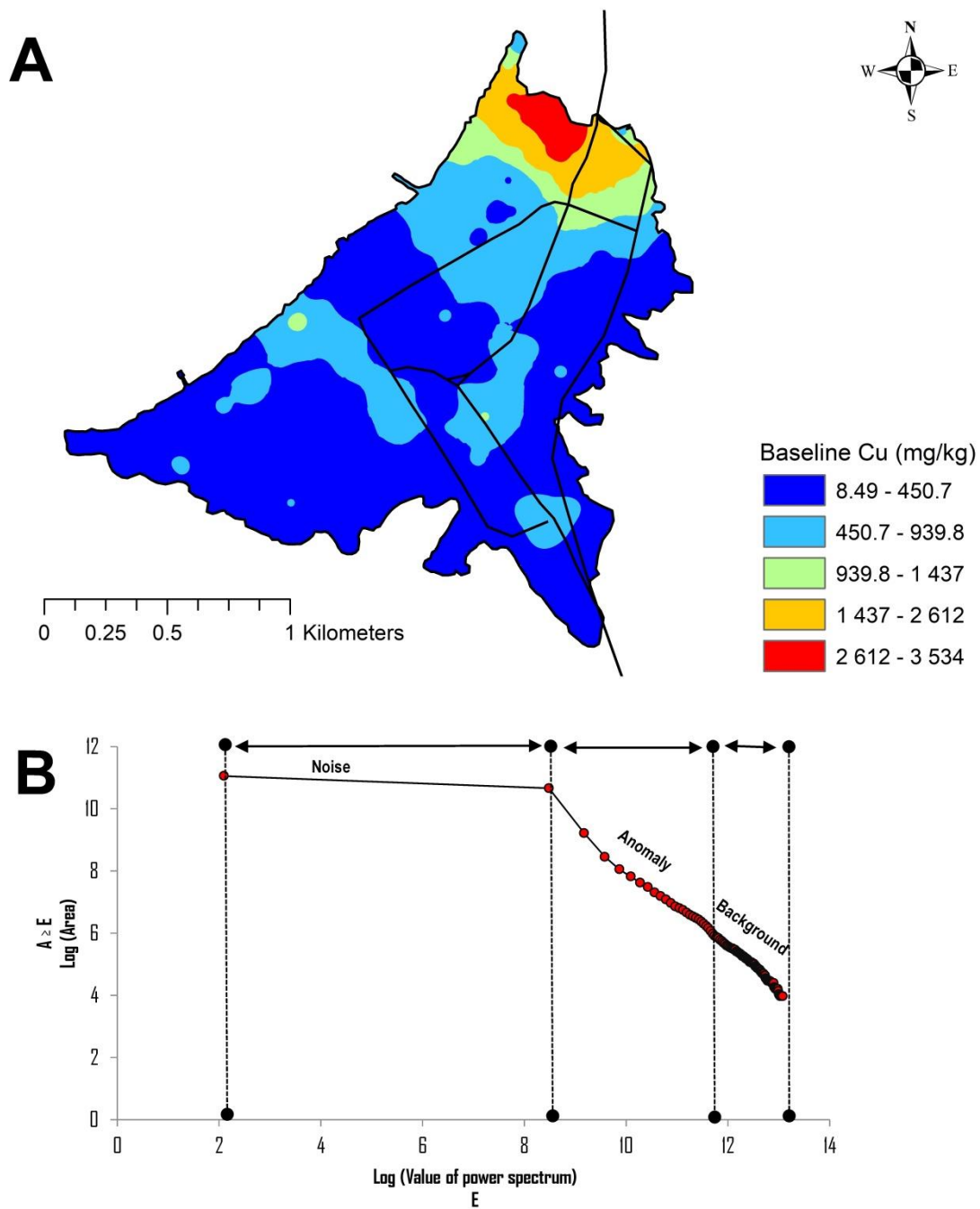


Figure 8.

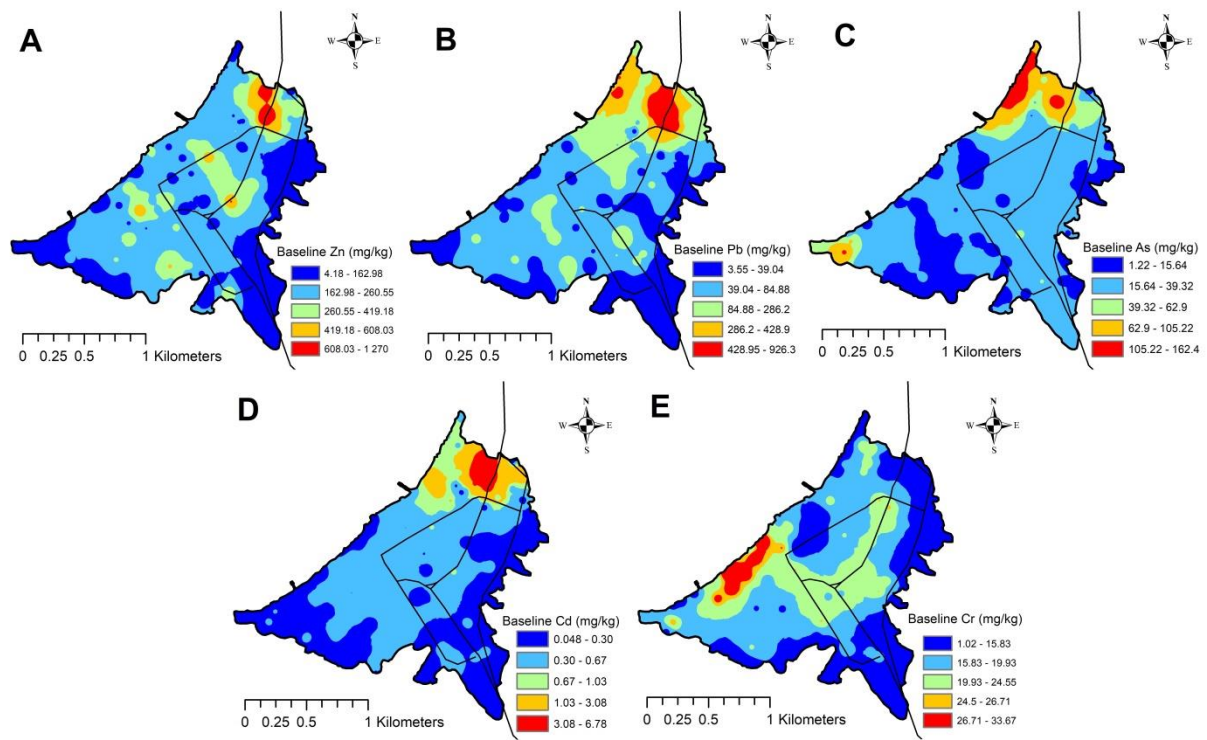


Figure 9.

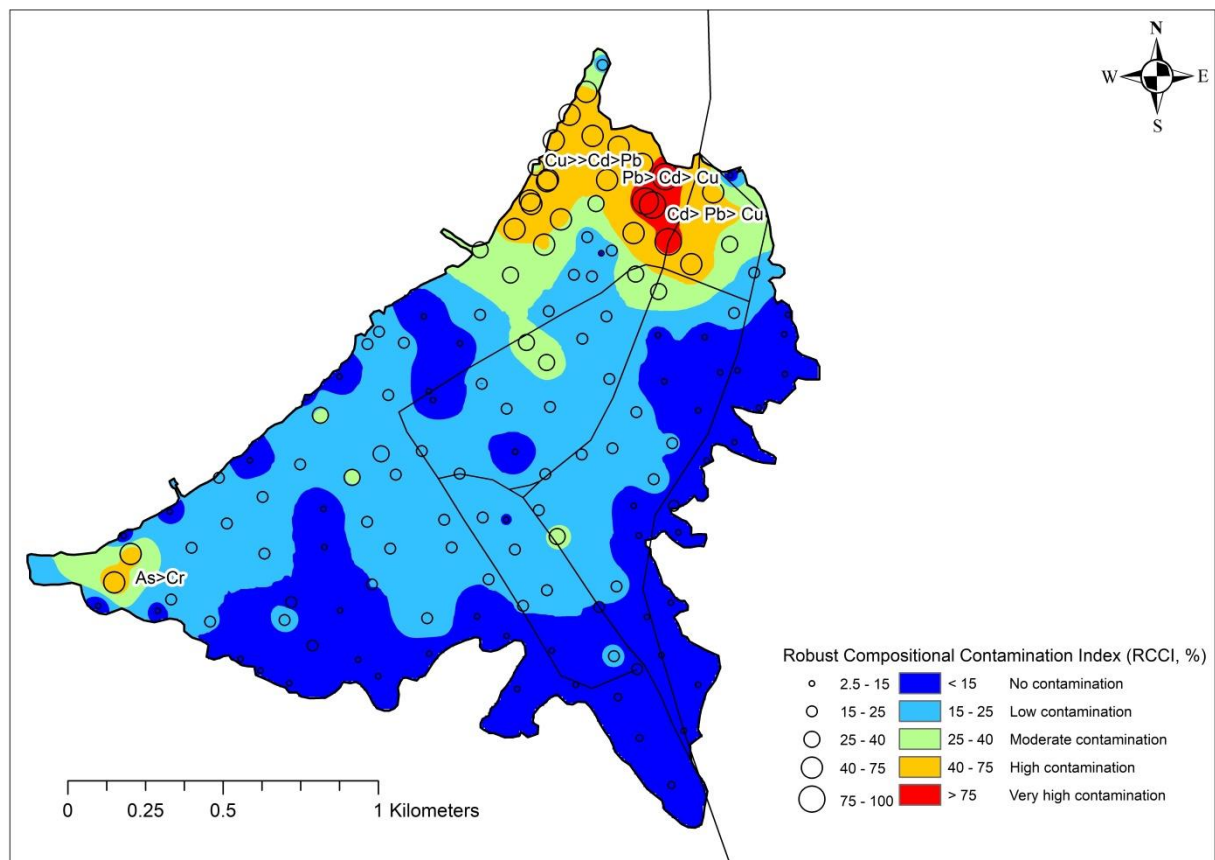


Table 1.

Elements	Unit	Detection limit (DL)	Accuracy (%)	Precision (%RPD)
Al	%	0.01	1.60	1.41
Ca	%	0.01	4.82	5.06
Fe	%	0.01	0.64	4.01
K	%	0.01	1.19	6.66
Mg	%	0.01	2.83	1.99
Na	%	0.01	4.55	8.32
Ti	%	0.01	0.12	7.49
Ag	mg/kg	0.2	3.57	3.12
As	mg/kg	2	2.86	13.91
Ba	mg/kg	10	13.33	7.49
Be	mg/kg	0.5	0	1.12
Cd	mg/kg	0.5	0.99	2.21
Co	mg/kg	1	3.85	9.31
Cr	mg/kg	1	6.82	11.44
Cu	mg/kg	1	2.97	10.87
Mn	mg/kg	5	1.50	2.10
Mo	mg/kg	1	22.70	0.79
Ni	mg/kg	1	5.00	4.03
Pb	mg/kg	2	2.01	10.50
Sb	mg/kg	2	5.59	13.01
Sc	mg/kg	1	0	3.85
Sr	mg/kg	1	3.90	10.62
V	mg/kg	1	0	7.95
Zn	mg/kg	2	2.87	5.87

Table 2.

Variable	Unit	Minimum	Maximum	Mean	Median	CV (%)	Std Deviation	Skewness	Kurtosis
Redox potential	mV	92.10	279	183.04	184.80	19.8	36.15	-0.05	-0.11
pH	-	6.86	9.89	7.91	7.88	7.5	0.59	0.44	0.27
EC (μ S/cm)	μ S/cm	13	109400	12550	8320	115.4	14483	2.83	13.37
Ag	mg/kg	0.1	10.9	0.65	0.3	180.2	1.16	5.83	43.49
Al	mg/kg	3700	35800	15756	14800	36.2	5704	0.88	1.07
As	mg/kg	5	345	37.85	18.85	149.6	56.63	3.21	10.27
Ba	mg/kg	20	1680	124.57	80	137.3	171.02	6.18	48.74
Be	mg/kg	0.25	1.10	0.40	0.46	41.9	0.17	1.06	1.75
Ca	mg/kg	3100	46100	19266	18800	38.0	7327	0.60	1.10
Cd	mg/kg	0.25	23	0.64	0.25	305.4	1.95	10.75	120.23
Co	mg/kg	8	77.10	20.58	17	58.3	11.99	2.43	6.34
Cr	mg/kg	2	87	19.26	18	46.5	8.96	3.60	23.26
Cu	mg/kg	39	6740	766.82	285	144.4	1107	2.58	7.51
Fe	mg/kg	23700	373000	54734	42500	82.3	45039	4.37	22.20
K	mg/kg	500	5800	2080	2000	40.6	843.88	0.91	2.23
Mg	mg/kg	2400	29200	13404	12600	38.3	5137	0.67	0.30
Mn	mg/kg	336	12850	865.44	670	158.2	1369	8.01	64.02
Mo	mg/kg	1	386	8.21	3.00	398.8	32.74	10.96	123.63
Na	mg/kg	300	37900	5714.37	4700	93.3	5333	2.49	9.83
Ni	mg/kg	2	192	21.05	14	118.8	24.99	4.10	19.68
Pb	mg/kg	8	2670	135.30	45.40	225.5	305.02	5.33	35.42
Sb	mg/kg	1	42.90	3.88	1	186.4	7.24	3.25	10.59
Sc	mg/kg	0.30	15	6.08	6	50.1	3.04	0.40	0.14
Sr	mg/kg	19	227	65.45	59	54.9	35.94	1.69	4.19
Ti	mg/kg	300	4000	1598.48	1315	50.9	814	0.96	0.41
V	mg/kg	58	663	120.97	105	59	71.31	4.78	27.80
Zn	mg/kg	45	2280	224.12	157	115.1	258.01	5.28	34.62

Table 3.

Location	Urban areas	As	Cd	Cr	Cu	Pb	Zn	Authors
South America								
Chile	Taltal	37.85	0.64	19.26	766.82	135.3	224.12	This study
Chile	Talcahuano	-	-	37.8	-	35.2	333	Tume et al. 2008
Brazil	Sau Paulo	9.64	49	-	-	-	81.5	Figueiredo et al. 2007
Asia								
China	Yibin City	10.55	-	-	51.63	61.23	138.88	Guo et al.2012
China	Hong kong		0.62	23.1	23.3	94.6	125	Li et al. 2004
Mongolia	Ulaanbaatar	14	0.8	20.3	35.9	63.9	158.7	Batjargal et al. 2010
Africa								
Nigeria	Ibadan metropolis	3.9	8.4	64.4	46.8	95.1	228.6	Odewande et al. 2006
Algeria	Annaba	-	0.44	30.9	39	53.1	67.5	Maas et al. 2010
Tunisia	Sfax	-	-	17.5	15.6	30.23	36.5	Wali et al. 2013
Europe								
Italy	Naples	12.4	0.5	12.5	163	100	142	Cicchella et al. 2005
Scotland	Glasgow	9		52	62	195	178	Ajmone-Marsan et al. 2008
Italy	Palermo	23	2	95.4	146.6	218.2	516	Manta et al. 2002

Table 4.

	Physico-chemical parameters			Elements					
	Redox	pH	EC	As	Cd	Cr	Cu	Pb	Zn
Redox				-0.3031	-0.2413	0.1664	-0.4776	-0.4933	-0.4259
pH				-0.5545	-0.4376	0.3251	-0.6583	-0.7356	-0.4722
EC				-0.1823	-0.2445	0.0935	-0.1333	-0.0931	-0.0748
As	0.0002***	0.00***	0.0299*		0.5081	-0.1294	0.6054	0.6873	0.0533
Cd	0.0038**	0.00***	0.0034**	0.00***		-0.2706	0.3769	0.6038	0.3899
Cr	0.0478*	0.0001***	0.2685	0.1248	0.0011**		-0.178	-0.2066	-0.2031
Cu	0.00***	0.00***	0.1137	0.00***	0.00***	0.0341*		0.6137	0.2278
Pb	0.00***	0.00***	0.2707	0.00***	0.00***	0.0136*	0.00***		0.4812
Zn	0.00***	0.00***	0.3765	0.5284	0.00***	0.0154*	0.0064**	0.00***	

* Significant correlation at p <0.05

** Significant correlation at p <0.01

*** Significant correlation at p <0.001

Table 5.

Variables	Factors				Communalities
	F1	F2	F3	F4	
Ag	0.76	0.10	-0.31	-0.19	0.72
Al	-0.85	0.00	-0.12	0.37	0.87
As	0.79	0.28	-0.03	0.17	0.74
Ba	0.22	-0.77	0.11	0.09	0.67
Be	-0.15	0.29	0.30	0.66	0.63
Ca	-0.65	-0.53	-0.03	0.04	0.71
Cd	0.70	-0.06	-0.30	0.35	0.71
Co	0.10	0.82	0.23	0.18	0.77
Cr	-0.04	-0.10	0.81	-0.22	0.72
Cu	0.65	0.38	-0.30	-0.32	0.75
Fe	0.21	0.73	0.51	0.17	0.86
K	-0.70	-0.50	-0.12	0.07	0.76
Mg	-0.85	-0.03	-0.12	0.33	0.84
Mn	-0.34	-0.03	-0.28	0.69	0.67
Mo	0.63	0.50	-0.08	-0.31	0.75
Na	-0.27	-0.50	0.08	-0.42	0.51
Ni	0.52	0.50	0.43	0.02	0.71
Pb	0.88	0.05	-0.16	-0.03	0.80
Sb	0.76	0.24	-0.15	0.32	0.77
Sc	-0.78	0.21	-0.18	-0.01	0.69
Sr	-0.25	-0.76	0.01	-0.09	0.65
Ti	-0.82	0.02	-0.11	0.28	0.77
V	-0.12	0.50	0.72	0.19	0.82
Zn	0.50	-0.39	-0.33	-0.12	0.53
Eigenvalues	9.15	4.42	2.21	1.39	
Total variance in %	34.18	18.34	10.02	8.67	
Cum. of total variance	34.18	53.03	63.05	71.73	

[Click here to view linked References](#)

Rebut

To the reviewers' comments on manuscript titled
**Source patterns of Potentially Toxic Elements (PTEs) and mining activity contamination level in
soils of Taltal city (Northern Chile)**

EGAH-D-19-00276R1

Arturo Reyes, Matar Thiombane, Antonio Panico, Linda Daniele, Annamaria Lima, Marcello Di Bonito, Benedetto
De Vivo

Dear Mr THIOMBANE,

We have received the reports from our advisors on your manuscript, "Source patterns of Potentially Toxic Elements (PTEs) and mining activity contamination level in soils of Taltal city (Northern Chile)", submitted to Environmental Geochemistry and Health.

Based on the advice received, I have decided that your manuscript can be accepted for publication after you have carried out the corrections as suggested by the reviewer(s).

Please respond to the reviewer's comments on a point-by-point basis indicating the page and line numbers where the amendments have been made, and highlighting the changes in the revised manuscript.

Attached, please find the reviewers' comments for your perusal.

With kind regards,

Springer Journal's Editorial Office

Environmental Geochemistry and Health

Reviewer's comments and authors responses

Dear Journal Editorial Officers,

First of all we would like to thank you for accepting the manuscript and appreciate the reviewer's comments and suggestions, which helped us to improve our paper substantially. As indicated below, we have checked all the general and specific comments provided by the reviewers and have made changes accordingly to their indications.

Kind regards,

Arturo Reyes, Matar Thiombane, Antonio Panico, Linda Daniele, Annamaria Lima, Marcello Di Bonito, Benedetto
De Vivo

Reviewer #1

This manuscript is a well-structure paper and can be published on this journal. I have minor comments and suggestions as below:

Comment (1): I was satisfied with this revision. However, the C-A and S-A fractal/multifractal models, and MIDW were used in this study. The state-of-art of these models should be introduced in the section of methods.

Response to comment (1): Dear reviewer, thank you for your comments. We have modified and complemented our manuscript based on your suggestions, by adding the materials that highlight state-of-art of the C-A and S-A fractal/multifractal, and MIDW models. See section 2.4.1. Spatial distribution and baseline values of PTEs (207 to 252).

Comment (2) Please note the similarity of your manuscript =35%. Could you please lower the similarity to about 20%?.

Response to comment (2): Thank you for your suggestions and the similarity is decrease as lower as possible. See new version of the manuscript.